with HIV-1, the cells were washed once with PBS containing 5 mM EDTA and twice with RPMI/FCS. Then, the cells were lysed with 150 μl of lysis buffer (20 mM Tris-HCl (pH 7.6), 150 mM NaCl, 5 mM $MgCl_2$, 0.2 mM phenylmethylsulfonyl fluoride, 5 μg/ml of aprotinin, 0.5% Triton X-100, and 7 mM 2-mercaptoethanol), and the cell lysates were centrifuged at 1000 × *g* for 2 min at 4 °C. Then, the concentration of HIV-1 $p24^{Gag}$ in the supernatants was determined by ELISA. The amount of $p24^{Gag}$ in these cell extracts was expressed as the total amount of viral $p24^{Gag}$ associated with the cells as described by Valenzuela *et al.* (41), because this value showed both viral $p24^{Gag}$ bound to the surface of cells and viral $p24^{Gag}$ that has entered the cells. To detect only HIV-1 that entered MOLT-4 cells, extracellular bound virus was removed. For this, cells were treated with 2.5 mg/ml of trypsin in PBS containing 5 mM EDTA for 40 s at room temperature after the cells were washed with PBS containing 5 mM EDTA. Then, the cells were washed twice with RPMI/FCS, lysed, and the concentration of intracellular $p24^{Gag}$ was determined by ELISA. As compared with a T-cell line, CEM cells, which have been reported to be treated with trypsin for 5 min (41), MOLT-4 cells were treated with it for 40 s because they were highly sensitive to trypsin.

Syncytium Formation Assay—MOLT-4/IIIB cells and C8166 cells were suspended in RPMI medium at 1×10^5 cells per ml and 5×10^5 cells per ml, respectively. Before addition of 50 μl of C8166 cell suspension to each well of a U-bottom 96-well plate (Corning), MOLT-4/IIIB cells (50 μl per well) were incubated with 100 μl of RPMI medium containing one of the synthetic peptides or the medium alone for 1 h at 37 °C. After incubation at 37 °C for 17 h, the number of syncytia per well was counted by light microscope observation (42). The inhibitory activity of peptide to syncytium formation (inhibition (%)) was calculated using the following formula: [(the number of syncytia with no peptide − the number of syncytia with peptide)/the number of syncytia with no peptide] × 100%.

Association of GPR1ntP-(1–27) with HIV-1 Virions—To concentrate virus particles (IIIB strain), the culture supernatant (10 ml) of MOLT-4/IIIB cells was layered onto a 20% (w/v) sucrose cushion (2.5 ml) and centrifuged at 100,000 × *g* for 2 h at 4 °C using a Hitachi SRP28 rotor (Hitachi Koki Co., Tokyo, Japan). The viral pellet was resuspended in 100 μl of TNE buffer (20 mM Tris-HCl (pH 7.5), 100 mM NaCl, 1 mM EDTA), layered onto the top of a continuous sucrose gradient (20–60% (w/v) sucrose in TNE) (43, 44), and centrifuged at 100,000 × *g* for 16 h at 4 °C. Fractions (700 μl) were collected from the top of the gradient, and the density of each fraction was determined. An aliquot from each fraction (50 μl) was mixed with 50 μl of TNE buffer containing 2% (v/v) Nonidet P-40 and 0.2% (w/v) bovine serum albumin, the mixture was incubated for 1 h at 56 °C, and the HIV-1 $p24^{Gag}$ protein was detected by dot blotting as described below. The fractions that contained HIV-1 virions were pooled, concentrated again by centrifugation at 100,000 × *g* for 2 h at 4 °C using an RP55S rotor (Hitachi Koki Co.), suspended in TNE buffer, and used for detection of the association of synthetic peptides (GPR1ntP-(1–27) or X4ntP-(1–28)) with the HIV-1 virions. The viral suspension (100 μl) was incubated with one of peptides (5 μg) for 1 h at 37 °C, subjected to sucrose density gradient sedimentation, and then fractionated. The dot blotting was carried out to detect the presence of the HIV-1 $p24^{Gag}$ protein and peptides in each fraction using anti-$p24^{Gag}$ mAb and anti-peptide antibodies, respectively.

Dot Blotting—The HIV-1 lysates prepared after sucrose density gradient ultracentrifugation were blotted onto nitrocellulose membranes (Schleicher & Schuell, Dassel, Germany) using a Minifol-Microsample Filtration Manifold (Schleicher & Schuell). They were then blocked with 5% nonfat dry milk (w/v) in PBS containing 0.1% Tween 20 (v/v) (PBST) (blocking buffer B) for 2 h at 37 °C. The membranes were then probed with α-$p24^{Gag}$ mouse mAb diluted 1:1000 with blocking buffer B, or anti-peptide antibodies (α-GPR1 or α-CXCR4; 2 μg/ml in blocking buffer B) for 1 h at room temperature. After being washed three times with PBST, the membranes were incubated with a horseradish peroxidase-labeled antibody to mouse or rabbit IgG (DAKO) diluted 1:1000 with blocking buffer B for 1 h at room temperature, and then washed three times. Immunoreactive spots were detected by the enhanced chemiluminescence (ECL) system (Amersham Biosciences) according to the manufacturer's instruction.

Detection of Binding of rgp120 to GPR1 Peptides by ELISA—The recombinant envelope glycoprotein (rgp120) of HIV-1 (IIIB strain) produced in a baculovirus expression system, >90% pure, was obtained from the AIDS Reagent Project of the United Kingdom Medical Research Council (Potters Bar, United Kingdom). ELISA to detect peptide-rgp120 or sCD4-rgp120 interaction was based on the protocol as described (45), with a few modifications. Wells of a 96-well microtiter plate (Corning) were coated with GPR1ntP-(1–27) or its fragment or mutant peptides (0.015–5 μM in PBS) for overnight at 4 °C, washed twice with PBS, and blocked with blocking buffer A for 2 h at room temperature. After being washed with PBS, rgp120 (0.016 μM) in PBS containing 1% (v/v) Triton X-100 was added, and the mixture was incubated for 2 h at room temperature and washed with PBST. To detect bound rgp120, anti-HIV-1 sera from AIDS patients diluted 1:2000 with 3% bovine serum albumin (w/v) in PBST (blocking buffer C) was added, and the mixture was incubated for 2 h at room temperature and washed with PBST. Then horseradish peroxidase-labeled antibody to human IgG diluted 1:5000 with blocking buffer C was added, and the mixture was incubated for 1 h at room temperature, washed with PBST, and rinsed with PBS. To develop color, 3,3′.5.5′-tetramethylbenzidine solution (Bio-Rad) as a substrate was added for 20 min at room temperature, and 1 N H_2SO_4 was added to stop the reaction. Then the optical densities (*A*) at 450 nm were determined.

For detection of interaction of sCD4 with GPR1ntP-(1–27), microtiter wells were coated with GPR1ntP-(1–27) as described above. Then, sCD4 (0.016 μM), which was obtained from the AIDS Reagent Project of the United Kingdom Medical Research Council, was added for 2 h at room temperature. Bound sCD4 was detected by ELISA as described above using antibody against sCD4 and horseradish peroxidase-labeled antibody to sheep IgG (Dako).

To examine the effect of α-GPR1 antibody on binding of GPR1ntP-(1–27) to rgp120, microtiter wells were coated with GPR1ntP-(1–27) as described above. Then purified α-GPR1 antibody or normal rabbit IgG (NRG) was added for 2 h at room temperature prior to addition of rgp120 (0.016 μM), and then bound rgp120 was detected as described above. For detection of binding of GPR1ntP-(1–27) to rgp120-sCD4, rgp120 (0.016 μM) was incubated with sCD4 (0.016 μM) for 1 h at 37 °C before incubation with GPR1ntP-(1–27) and then bound rgp120 was detected as described above. For detection of the binding of rgp120 to GPR1ntP-(1–27) or sCD4 in the presence of heparin (Wako), microtiter wells were coated with either GPR1ntP-(1–27) (1.0 μM) or sCD4 (0.016 μM) as described, and rgp120 (0.016 μM), which had been preincubated with or without heparin (37 °C for 1 h) was added. Bound rgp120 was detected as described above.

To examine the effect of GPR1ntP-(1–27) on binding of V3-specific neutralizing mouse mAb (0.5β) to rgp120, a microtiter plate was coated with rgp120 (0.016 μM) at 4 °C for overnight, blocked, and treated with or without different concentrations of GPR1ntP-(1–27) or X4ntP-(1–28) (5–100 μM) at room temperature for 2 h. After being washed with PBS, mAb 0.5β (ascites, 1:500 dilution) was added, and the plate was incubated at room temperature for 2 h, and washed. Captured 0.5β was detected as described above using a horseradish peroxidase-labeled antibody to mouse IgG (Dako).

RESULTS

Effects of Synthetic Peptides Derived from the NH_2-ECR of GPCRs on Cell-free HIV-1 Infection—We have previously established human glioma-derived, new HIV-1 infection indicator cell lines, which are transduced with both CD4 and co-receptors (NP-2/CD4/GPCRs), and showed that infectivity assay using these cell lines were highly reproducible and sensitive (13–15, 22, 23). As shown in Fig. 1, detection of HIV-1 antigen-positive cells by immunostaining after infection with several HIV-1 strains is dependent on both CD4 and the types of co-receptors expressed on NP-2 cells.

We, therefore, examined the effects of synthetic peptides derived from NH_2-ECR of GPCRs (GPR1, CXCR4, CCR3, and CCR5) on the infectivity of several HIV-1 strains by focal infectivity assays with NP-2/CD4/GPCRs as indicator cells (Fig. 2). Because our initial experiments indicated that the treatment of cells with the peptides at 37 °C for 1 h and their removal by washing before virus inoculation did not affect the infectivity by HIV-1, virus was incubated with one of the peptides (37 °C for 1 h), and this virus-peptide mixture was added to target cells. Among the peptides, only GPR1ntP-(1–27) markedly inhibited the infection of NP-2/CD4/GPR1 cells with GUN-1Ser strain, which utilizes GPR1 as a co-receptor, in a dose-dependent manner. Surprisingly, infections of the IIIB (X4), GUN-1WT (R5X4), and BaL (R5) strains were also inhibited by GPR1ntP-(1–27). As for IIIB, GUN-1Ser, and GUN-1WT strains, 50% inhibitory concentrations (IC_{50}) were 0.4–

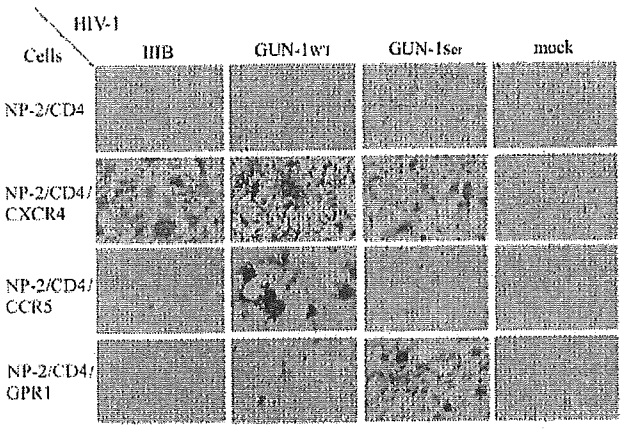

FIG. 1. **Infection of NP-2/CD4/GPCRs cells with HIV-1.** The CD4-transduced NP-2 cells (NP-2/CD4) and those stably expressing GPCRs (CXCR4, CCR5, and GPR1) were infected with HIV-1 (IIIB, GUN-1WT, and GUN-1Ser strains), fixed with methanol at 2 days later, and stained for HIV-1 antigen-positive cells. Stained cells were photographed by light microscope (×200).

0.8 μM and 90% inhibitory concentrations (IC_{90}) were 3–12 μM (Table II), whereas GPR1ntP-(1–27) had weaker effects on infection of R5 virus (BaL strain) as compared with other HIV-1 strains; its IC_{50} and IC_{90} were 10 μM and 50 μM, respectively. No inhibitory activities of X4ntP-(1–28), R3ntP-(1–24), and R5ntP-(1–20) against any HIV-1 strains tested were detected. As for R5ntP-(1–20), our results are consistent with previous reports showing that no inhibitory effects on HIV-1 infection are detected in unmodified synthetic peptides derived from the NH_2-ECR of CCR5 (46, 47).

Effect of GPR1ntP-(1–27) on the Infection of HIV-1 Primary Isolates—We next examined the effect of GPR1ntP-(1–27) on the infection of primary R5X4-tropic HIV-1 strains, GUN-4 and GUN-14, which had been isolated from Japanese hemophilia patients. For this, the viruses were mixed with or without GPR1ntP-(1–27) and inoculated onto NP-2/CD4/CCR5 cells. The concentration of $p24^{Gag}$ protein in culture supernatants at 3 days after inoculation was measured (Fig. 3). GPR1ntP-(1–27) inhibited infection of both primary GUN-4 and GUN-14 strains in a dose-dependent manner. In addition to primary isolates, we also examined the effect of GPR1ntP-(1–27) on the infection of R5-tropic SF162 strain. Infection of SF162 strain was inhibited by GPR1ntP-(1–27) in a dose-dependent manner at higher concentrations, but this strain, like BaL strain, was relatively resistant to GPR1ntP-(1–27). Thus, as summarized in Table II, the inhibitory activities of GPR1ntP-(1–27) against HIV-1 strains (IIIB, GUN-1WT, GUN-1Ser, GUN-4, and GUN-14) that can utilize CXCR4 as their co-receptors were 10–20 times as strong as R5 viruses (BaL and SF162). No inhibitory activity of a synthetic peptide derived from the NH_2-ECR of CCR5, R5ntP-(1–20), to infection of all HIV-1 strains, including primary strains, was repeatedly detected.

Inhibition of HIV-1 Infectivity to a T-cell Line and Primary PBLs by GPR1ntP-(1–27) at Early Infection Step before Reverse Transcription—We next examined which step of virus infection was inhibited by GPR1ntP-(1–27). For this, a human T-cell line, MOLT-4, was infected with cell-free HIV-1 (IIIB strain), DNA was harvested 20 h after infection, and then the synthesis of HIV-1 DNA in target cells was detected by PCR using primers specific for the *gag* region. The relative intensities of amplified DNA bands were correlated with dilutions of the inoculated virus, indicating that PCR was performed within a linear range (Fig. 4, *A* and *B*). When HIV-1 was inoculated into the target cells in the presence of GPR1ntP-(1–27), the formation of HIV-1 DNA was inhibited in a dose-dependent manner (Fig. 4, *C*, lanes 1–5, and *D*). The inhibitory activity was not again detected when X4ntP-(1–28), R3ntP-(1–24), or R5ntP-(1–20) was used (Fig. 4, *C*, lanes 6–8 and *D*). When GPR1ntP-(1–27) was added to MOLT-4 cells only after inoculation of the virus, the formation of HIV-1 DNA was not inhibited (data not shown), suggesting that the reverse transcription of HIV-1 RNA in the host cells was not inhibited by GPR1ntP-(1–27).

We next examined whether GPR1ntP-(1–27) could inhibit HIV-1 infection to primary human PBLs, which are natural targets for HIV-1. The formation of reverse-transcribed HIV-1 DNA in PBLs, prepared from two independent donors, was also clearly inhibited by GPR1ntP-(1–27) in a dose-dependent manner (Fig. 4, *E* and *F*). Thus, these findings indicate that GPR1ntP-(1–27) blocks the early step of HIV-1 infection before reverse transcription, such as virus attachment or its entry into target cells.

Effect of GPR1ntP-(1–27) on Syncytium Formation—To examine the effect of GPR1ntP-(1–27) on the formation of multinucleated giant cells (syncytia), which are considered to represent cell-to-cell infection, we performed syncytia assays using HIV-1-positive MOLT-4/IIIB cells and HIV-1-negative C8166 cells in the presence of one of the synthetic peptides (Fig. 5). Syncytium formation was clearly inhibited by GPR1ntP-(1–27) but not by the other peptides. IC_{50} of GPR1ntP-(1–27) determined by the syncytia assay was 1.1 μM. Because little effect of 50 μM GPR1ntP-(1–27) on the growth and viability of MOLT-4 cells was observed for up to 4 days (data not shown), the anti-HIV-1 activity of GPR1ntP-(1–27) appears not to be due to its cell toxicity.

Identification of a Functional Domain and Amino Acids in GPR1ntP-(1–27) Responsible for Its Anti-HIV-1 Activity—To determine a functional domain in the GPR1ntP-(1–27) peptide more precisely, fragment peptides, overlapped by six amino acids (GPR1ntP-(1–13), GPR1ntP-(8–20), and GPR1ntP-(15–27)) were synthesized (Table I). We examined the effect of these fragment peptides on the infection of NP-2/CD4/GPCR cells with HIV-1 (IIIB, GUN-1Ser, and BaL strains) (Table III). Among a series of the fragment peptides, GPR1ntP-(15–27) inhibited the infection of the IIIB and GUN-1Ser strains but not that of the BaL strain. Although relatively high concentrations of GPR1ntP-(15–27) were required for the inhibition of HIV-1 infection as compared with GPR1ntP-(1–27), the inhibitory effect of GPR1ntP-(15–27) against HIV-1 was repeatedly detected. This result indicates that the amino acid sequence from 15 to 27 (YSYDLDYYSLESC) is pivotal to inhibit HIV-1 infection by GPR1ntP-(1–27). Because it has been implicated that the tyrosine residues in the NH_2-ECR of CXCR4 and CCR5 play an important role in the co-receptor activity for HIV-1 infection (16–21), we examined a mutant peptide, in which all tyrosine residues had been substituted with alanine residues (GPR1ntP-(Y/A); Y15A, Y17A, Y22A, and Y23A), on HIV-1 infection. The inhibitory activity of GPR1ntP-(Y/A) peptide against HIV-1 infection was completely abrogated, indicating that tyrosine residues play a crucial role for GPR1ntP-(1–27) to inhibit HIV-1 infection.

Binding of GPR1ntP-(1–27) to Highly Purified HIV-1 Virions—Because no inhibitory effect of GPR1ntP-(1–27) was detected when cells had been treated with GPR1ntP-(1–27) and washed before HIV-1 inoculation, it is most likely that targets for GPR1ntP-(1–27) are virus particles rather than the host cell molecules. To test this, we performed a GPR1ntP-(1–27)-binding assay using HIV-1 virions highly purified through sucrose density gradient ultracentrifugation. The purified virus (IIIB strain) was incubated with GPR1ntP-(1–27) for 1 h at 37 °C, subjected to sucrose density gradient sedimentation, and then

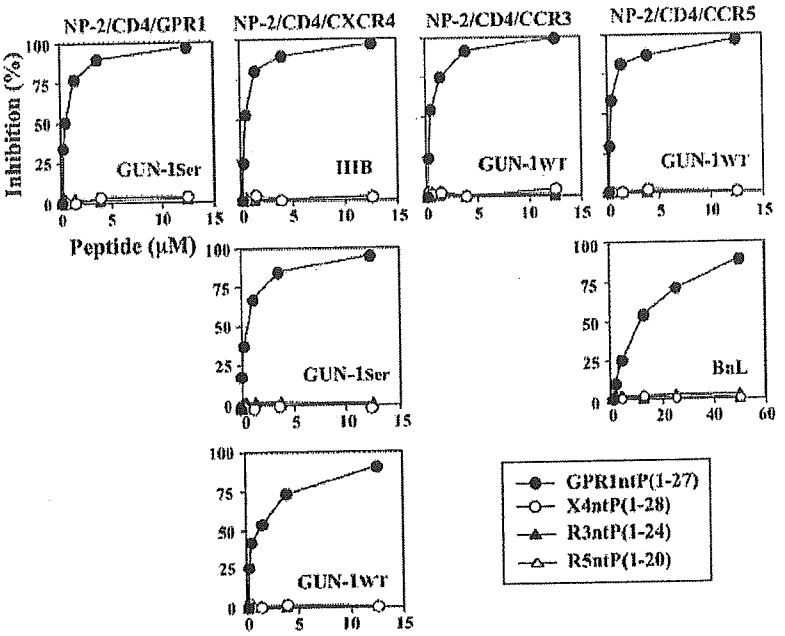

FIG. 2. **Inhibition of cell-free HIV-1 infection by GPR1ntP-(1–27).** NP-2/CD4 cells expressing one of the GPCRs were infected with HIV-1 in the presence or absence of synthetic peptides derived from the NH_2-ECR of GPCRs, and HIV-1-antigen-positive cells were detected by focal infectivity assay as described under "Experimental Procedures." The target cell and inoculated HIV-1 strain are indicated at the *top of graph* and within the graph, respectively. The average number of foci in triplicate wells formed in the presence of peptides was counted, and the inhibition (%) was determined by the comparison with the average number of foci formed in the absence of peptides (~500 foci/well). Four independent experiments gave similar results.

TABLE II
Inhibition of HIV-1 infection by GPR1ntP-(1–27)

Strain	Coreceptor	IC_{50}[a]	IC_{90}[a]
		μM	
IIIB	CXCR4	0.5	4.0
GUN-1ser	CXCR4	0.4	4.0
	GPR1	0.5	6.0
GUN-1WT	CXCR4	0.8	12.0
	CCR3	0.45	3.0
	CCR5	0.5	6.0
GUN-4[b]	CXCR4	ND[c]	ND
	CCR5	0.6	6.5
GUN-14[b]	CXCR4	ND	ND
	CCR5	0.2	2.0
BaL	CCR5	10.0	50.0
SF162	CCR5	5.0	33.0

[a] IC_{50} and IC_{90} of the GPR1ntP-(1–27) for each HIV-1 strain were determined by focal infectivity assay using NP-2/CD4/GPCR cells in comparison with the number of foci induced by each HIV-1 strain without a peptide. As for GUN-4, GUN-14, and SF162 strains, IC_{50} and IC_{90} were determined by measuring the concentrations of p24 in the culture supernatants by ELISA.

[b] The primary HIV-1 strains isolated from Japanese hemophilia patients.

[c] ND, not determined.

the HIV-1 protein and GPR1ntP-(1–27) in each fraction were detected by dot spotting (Fig. 6). The sedimentation of virions with or without GPR1ntP-(1–27) was mainly detected in *fractions #8* and *#9* (Fig. 6*A*, the *first* and *second blots*), consistent with an expected density for retroviruses (~1.15 g/ml) (43, 44) (Fig. 6*B*), indicating that the presence of GPR1ntP-(1–27) did not affect the sedimentation of the virions. Sucrose density gradient sedimentation of GPR1ntP-(1–27) without virions revealed that this peptide remained at the top of the gradient (*#1* and *#2*), and it was hardly detectable in the fractions at densities around 1.15 g/ml (*#8* and *#9*) (the *third dot blot*). In contrast, when GPR1ntP-(1–27) had been mixed with HIV-1 before sedimentation, this peptide was detected not only in the *top fractions* (*#1* and *#2*) but also in the *middle fractions* (mainly in *#8* and *#9*) containing viral particles (the *fourth dot blot*), indicating co-sedimentation of HIV-1 virions and GPR1ntP-(1–27). This was confirmed by measuring the intensity of signal in *each dot spot* (*fractions #5–#11*) (Fig. 6*B*). The interaction of GPR1ntP-(1–27) with the virions is specific for GPR1ntP-(1–27) sequence, because the co-sedimentation of X4ntP-(1–28) with the virions was hardly detectable in the *middle fractions* (*#8* and *#9*, the *fifth blot*). Thus, these results indicated that GPR1ntP-(1–27) specifically associates with HIV-1 virions (IIIB strain) under physiological conditions.

Specific Interaction of GPR1ntP-(1–27) with rgp120 through Its V3 Loop—We next examined whether GPR1ntP-(1–27) binds directly to envelope glycoprotein gp120. Because GPR1ntP-(1–27) efficiently inhibited infection of X4 HIV-1 (IIIB strain), we performed a binding assay using a baculovirus-derived recombinant gp120 (rgp120) (IIIB strain) and GPR1ntP-(1–27). Microtiter plate wells were coated with different concentrations of GPR1ntP-(1–27) (0.015–5 μM) and incubated with rgp120 (0.016 μM), and bound rgp120 was detected by ELISA (Fig. 7*A*). The binding of rgp120 to GPR1ntP-(1–27) was detected in a concentration-dependent manner, indicating an association of rgp120 with GPR1ntP-(1–27). This binding appears to be specific, because pretreatment of GPR1ntP-(1–27) with α-GPR1, which had been generated by immunization of rabbits with GPR1ntP-(1–27), but not with normal rabbit IgG inhibited binding of rgp120 in a manner dependent on IgG concentrations (Fig. 7*B*). In contrast to rgp120, no binding of sCD4 to GPR1ntP-(1–27) was detected (Fig. 7*A*).

It is known that the CD4-binding domain (CD4-bd) and the V3 loop within gp120 play an important role for its interaction with target cells at the entry step of virus infection. To determine which region in rgp120 is involved in its binding to GPR1ntP-(1–27), we firstly examined the effect of sCD4 on the binding of rgp120 to GPR1ntP-(1–27) (Fig. 7*C*). When rgp120 had been incubated with sCD4 before addition to GPR1ntP-(1–27), sCD4 did not affect the binding of rgp120 to GPR1ntP-(1–27), suggesting that the CD4-bd in rgp120 might not be involved in the primary binding site for GPR1ntP-(1–27).

Because it has been reported that the soluble polyanion such as heparin binds to rgp120 at the V3 loop region (48–50), we next examined the effect of heparin on binding of rgp120 to GPR1ntP-(1–27) (Fig. 7*D*). The rgp120 was incubated with different concentrations of heparin (37 °C for 1 h) before addition to microtiter wells, which had been coated with either GPR1ntP-(1–27) or sCD4, and bound rgp120 was detected by ELISA. We found that heparin could inhibit association of

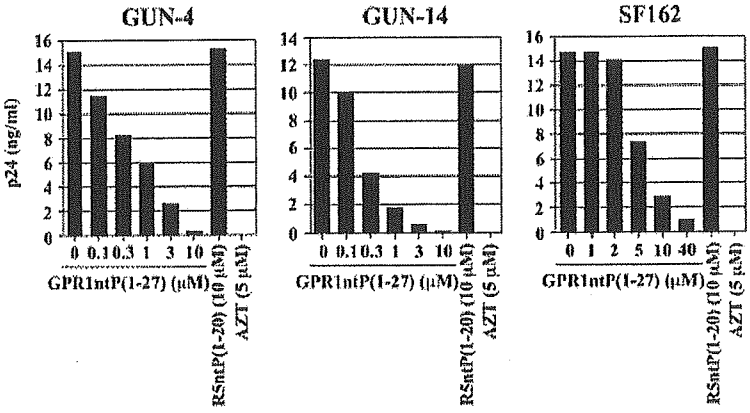

FIG. 3. **Effect of GPR1ntP-(1–27) on the infectivity of HIV-1 primary isolates.** NP-2/CD4/CCR5 (4×10^5) cells were infected with one of R5X4-tropic HIV-1 primary isolates (GUN-4 or GUN-14) or R5-tropic SF162 strain (each 10 ng of $p24^{Gag}$) in the presence or absence of GPR1ntP-(1–27) or R5ntP-(1–20). Then, $p24^{Gag}$ in culture supernatants at 3 days after infection were measured by ELISA. As a control, 5 μM azido-3′-deoxythymidine was added. Data are means obtained from duplicate samples. Experiments were repeated three times to confirm results.

rgp120 with GPR1ntP-(1–27) in a concentration-dependent manner. In contrast, heparin had little effect on the binding of sCD4 to rgp120, which is in consistent with a previous report (49).

To examine whether the V3 loop in rgp120 is involved in binding to GPR1ntP-(1–27), we carried out binding assays using the mAb, 0.5β, which has been reported to recognize the V3 loop of the IIIB strain (31). Microplate wells were coated with rgp120, incubated with 0.5β, and bound 0.5β was detected by ELISA (Fig. 7*E*). Incubation of rgp120 with GPR1ntP-(1–27) before addition of 0.5β resulted in inhibition of 0.5β binding to rgp120 in a concentration-dependent manner, whereas X4ntP-(1–28) did not have much of an effect at any concentrations tested. Taken together, these results strongly suggested that the V3 loop plays an important role for binding of GPR1ntP-(1–27) to rgp120.

To determine which region of GPR1ntP-(1–27) was necessary for rgp120 binding, we next examined the binding activities of the fragment peptides to rgp120 (Fig. 7*F*). Among the fragment peptides, a small peptide, GPR1ntP-(15–27) significantly bound to rgp120, with a lower affinity compared with GPR1ntP-(1–27), which is consistent with our finding that GPR1ntP-(15–27) inhibited HIV-1 infection at higher concentrations (Table III). In contrast, any apparent interaction of neither GPR1ntP-(1–13) nor GPR1ntP-(8–20) with rgp120 was detected. The tyrosine mutant GPR1ntP-(Y/A) completely lost its ability to bind to rgp120, indicating that tyrosine residues in GPR1ntP-(1–27) play an important role in its binding to rgp120 as well as in its inhibition of HIV-1 infection (Table III).

Inhibition of HIV-1 Binding to MOLT-4 Cells by GPR1ntP-(1–27)—It has been reported that the V3 loop is exposed on the surface of intact virions (52, 53). In addition, it has also been reported that anti-V3 loop mAbs inhibit the binding of HIV-1 to cells (41), suggesting that the V3 loop exposed on the surface of virion plays an important role for its binding to the target cells. Since our sucrose density gradient sedimentation assay indicated that GPR1ntP-(1–27) bound to intact virions (Fig. 6), and the ELISA assay revealed that there was a specific interaction between the V3 loop and GPR1ntP-(1–27) (Fig. 7), we examined whether GPR1ntP-(1–27) affected the binding of HIV-1 (IIIB strain) to MOLT-4 cells. For this, the cells were incubated with HIV-1 at 37 °C for 1 h, washed three times, and lysed, and the total amount of viral p24 core protein associated with the cells was determined by ELISA. The effects of anti-human CD4 mAb (NU-TH/I), anti-V3 loop mAb (0.5β), and heparin on the binding of HIV-1 to MOLT-4 cells at a concentration of 10 μg/ml were firstly examined. At this concentration, we confirmed that these anti-HIV-1 reagents inhibited infection of MOLT-4 cells with HIV-1 (IIIB strain) by more than 95% (data not shown). Even when MOLT-4 cells were treated with NU-TH/I before inoculation of virus, 1670 pg of $p24^{Gag}$ (58.8% of control) was still detected to be bound to the cells (Fig. 8*A*). To distinguish whether this $p24^{Gag}$ was derived from the extracellular viruses bound to the surface of the cells or from intracellular viruses that entered the cells, the cells were treated with trypsin to remove the former fraction of viruses (Fig. 8*B*). The result showed that viral $p24^{Gag}$ protein was hardly detectable after trypsin treatment, indicating that it was derived from the viruses bound to the surface of NU-TH/I-treated MOLT-4 cells. In agreement with a previous report (41), our findings suggested that HIV-1 was associated with not only CD4, but also with sites other than CD4 on the surface of MOLT-4 cells.

In contrast to anti-CD4 mAb (NU-TH/I), incubation of viruses with 0.5β or heparin before inoculation of viruses blocked the binding of HIV-1 to MOLT-4 cells almost completely (Fig. 8*A*), suggesting that the V3 loop contributed for the binding of HIV-1 to MOLT-4 cells. Interestingly, the binding of HIV-1 to MOLT-4 cells was also inhibited to a similar extent by GPR1ntP-(1–27) at a concentration of 20 μM: PCR assay showed the same concentration of GPR1ntP-(1–27) similarly inhibited the entry of HIV-1 (IIIB strain) to MOLT-4 cells (Fig. 4, *C* and *D*). A mutant peptide substituting all tyrosine residues in GPR1ntP-(1–27) to alanine, GPR1ntP-(Y/A), did not affect the binding of HIV-1 to cells at the same concentration. As expected, intracellular viral $p24^{Gag}$ was hardly detectable (Fig. 8*B*) when viruses were treated with 0.5β, heparin, or GPR1ntP-(1–27) prior to inoculation. GPR1ntP-(Y/A) again had hardly any effect on HIV-1 entry. Thus, these findings strongly suggested that the inhibition of binding of HIV-1 to MOLT-4 cells by GPR1ntP-(1–27) might be due to its interaction with the V3 loop exposed on the surface of intact virions.

DISCUSSION

In this study, we found that the 27-amino acid-long synthetic peptide derived from the NH_2-ECR of GPR1 inhibits HIV-1 infection of human glioma-derived indicator cells (NP-2/CD4/GPCRs), a T-cell line, and more importantly, primary PBLs, which are natural targets for HIV-1 infection. The inhibitory effect of GPR1ntP-(1–27) was observed not only in GUN-1Ser strain, which utilizes GPR1 as a co-receptor, but also in diverse HIV-1 strains, including X4 (IIIB), R5X4 (GUN-1WT, GUN-4, and GUN-14), and R5 (BaL and SF162) (Figs. 2 and 3 and Table II). Among these HIV-1 strains tested, R5 viruses were relatively resistant to GPR1ntP-(1–27) as compared with the other strains.

We found that GPR1ntP-(1–27) binds to rgp120 (Fig. 7, *A* and *B*), and this interaction is inhibited by heparin (Fig. 7*D*), which has been reported to bind to the V3 loop of gp120 (48–50). Moreover, interaction between anti-V3 loop mAb (0.5β) with rgp120 was inhibited by GPR1ntP-(1–27) (Fig. 7*E*). Be-

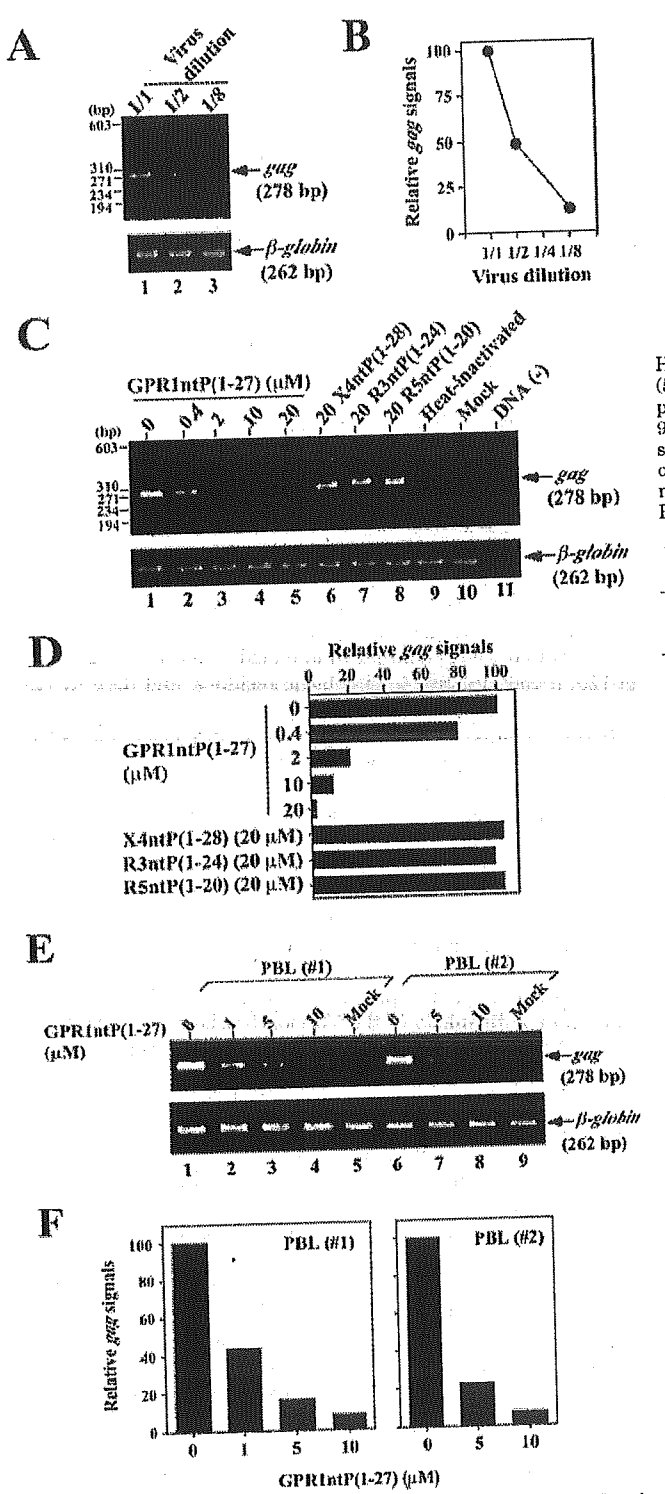

FIG. 4. **Inhibition of HIV-1 infectivity to T-cell line and primary PBLs by GPR1ntP-(1–27).** *A*, detection of reverse-transcribed HIV-1 (IIIB strain) DNA by PCR. Human T-cell line, MOLT-4 cells, were inoculated with serially diluted HIV-1, lysed 20 h after inoculation, and examined by PCR using the primers specific for the HIV-1 *gag* region (*lanes 1–3*). Amplification of β-globin was performed as a control. *B*, the intensity of signal in each lane was measured by a densitometer. Then the relative intensity of *gag* signal was determined by dividing the intensity of viral *gag* DNA by that of β-globin DNA and plotted. *C*, dose-dependent inhibition of HIV-1 infection by GPR1ntP-(1–27). MOLT-4 cells were infected with HIV-1 in the presence of one of the synthetic peptides derived from the NH_2-ECR of GPCRs (*lanes 1–8*). Formation of HIV-1 DNA in MOLT-4 cells was detected by PCR as described above. MOLT-4 cells were infected with heat-inactivated (56 °C, 30 min) HIV-1 (*lane 9*). *Lane 10* is a mock-infected control. PCR amplification was performed without template DNA (*lane 11*). β-Globin DNA was amplified as a control to confirm the efficiency of the amplification of each sample. *D*, the intensity of DNA signal in each lane was measured and the relative intensity of *gag* signal was determined as described above. *E*, inhibition of HIV-1 infection to primary human PBLs by GPR1ntP-(1–27). Primary PBLs prepared from two independent donors (*PBL#1* and *PBL#2*) were infected with HIV-1 (IIIB strain) in the presence or absence of GPR1ntP-(1–27). Formation of reverse-transcribed HIV-1 *gag* DNA in PBLs was detected by PCR as described above. *F*, the intensity of DNA band in each lane was measured, and the relative intensity of *gag* signal was determined as described above. Three independent experiments gave similar results.

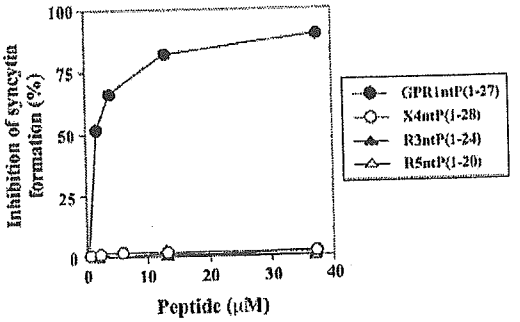

FIG. 5. **Inhibition of syncytium formation by GPR1ntP-(1–27).** HIV-1-negative C8166 (2.5×10^4) cells were incubated with MOLT-4 (5×10^3) cells chronically infected with HIV-1 (IIIB strain) in the presence or absence of one of the synthetic peptides for 17 h at 37 °C in 96-well plates in 200 μl of culture medium. At that time, the number of syncytia was counted by microscopic examination. The inhibitory effect of each peptide (%) was calculated in comparison with the average number of syncytia (~200) of triplicate control wells (no peptide added). Experiments were repeated three times to confirm results.

TABLE III
Effects of fragment and mutant GPR1 peptides on HIV-1 infection

Peptide[a]	Strain[b]		
	IIIB	GUN-1ser	BaL
		μM[c]	
GPR1ntP-(1–27)	0.5[c]	0.5	10
GPR1ntP-(1–13)	>100	>100	>100
GPR1ntP-(8–20)	>100	>100	>100
GPR1ntP-(15–27)	90	70	>100
GPR1ntP-(Y/A)	>100	>100	>100

[a] Amino acid sequence of each peptide is shown in Table I.
[b] NP-2/CD4/CXCR4, NP-2/CD4/GPR1, and NP-2/CD4/CCR5 cells were used for infection with IIIB, GUN-1Ser, and BaL strains, respectively.
[c] IC_{50} values (μM) of peptides were determined by focal infectivity assay; the number of foci induced by each HIV-1 strain in the presence and absence of a peptide was counted.

cause it has been reported that 0.5β recognizes 24 amino acids (308–331) of the V3 loop (31) and does not block binding of gp120 to CD4 (54), our data strongly suggested that the V3 loop plays an important role for binding of GPR1ntP-(1–27) to rgp120.

GPR1ntP-(1–27) inhibited binding of 0.5β to rgp120 by 50% at 25 μM, although the peptide at higher concentrations up to 100 μM showed only a limited decrease in rgp120 binding (Fig. 7*E*). As for the affinity of 0.5β for rgp120, an A_{450} value of binding of GPR1ntP-(1–27) at 0.6 μM to rgp120 was 0.32 (Fig. 7*A*), whereas almost a similar A_{450} value was obtained when 0.027 μM of 0.5β was used (data not shown), suggesting that the affinity of 0.5β for rgp120 is 22 times as high as that of GPR1ntP-(1–27). Thus, the incubation of 0.5β with rgp120 may displace GPR1ntP-(1–27) from rgp120 through a competitive

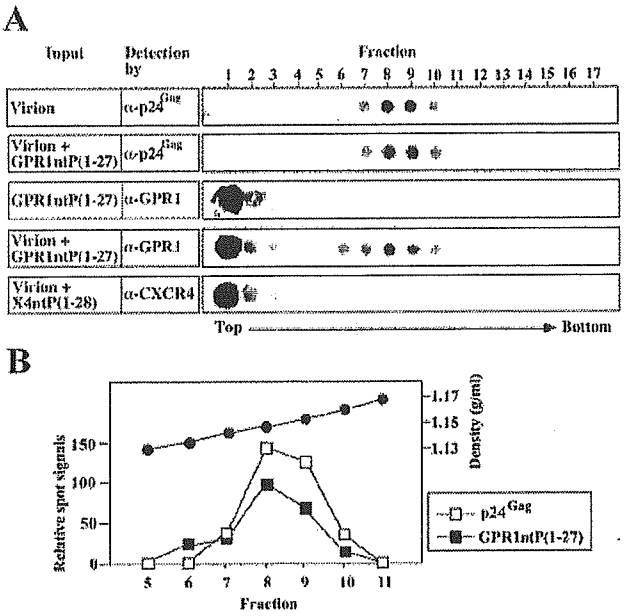

FIG. 6. **Binding of GPR1ntP-(1–27) to the highly purified HIV-1 virions.** *A*, culture supernatants of MOLT-4/IIIB cells were concentrated to pellet virions through a 20% sucrose cushion (100,000 × *g* for 2 h). The virus suspension was then subjected to a 20–60% sucrose density gradient sedimentation (100,000 × *g* for 16 h). Virus-containing fractions were concentrated, resuspended in TNE buffer (20 mM Tris-HCl (pH 7.5), 100 mM NaCl, 1 mM EDTA), and incubated with the GPR1ntP-(1–27) or X4ntP-(1–28) for 1 h at 37 °C. The virus, virus-peptide mixture or peptide (indicated as input) was then subjected to 20–60% sucrose density gradient sedimentation (100,000 × *g* for 16 h). Fractions (700 μl) were collected from the top of the gradient. The dot blotting was carried out to detect the presence of the HIV-1 $p24^{Gag}$, GPR1ntP-(1–27), and X4ntP-(1–28) in each fraction using α-$p24^{Gag}$, α-GPR1, and α-CXCR4, respectively. The exposure time for α-$p24^{Gag}$ dot blots (the first and second dot blots) were 1 min, and that for α-GPR1 dot blots (the *third* and *fourth dot blots*), and for α-CXCR4 dot blot (the *fifth dot blot*) were 10 min. *B*, the density of each fraction was measured and plotted (*fractions #5–#11*) (*closed circles*). The intensity of signal in each *dot spot* (*#5–#11*) ($p24^{Gag}$ of the *second dot blot* (*open squares*) and GPR1ntP-(1–27) of the *fourth dot blot* (*closed squares*)) was measured by a densitometer, and relative spot signals were plotted.

action of 0.5β for rgp120, and this may explain a slight and limited decrease in 0.5β binding to rgp120 even in the presence of high concentrations of GPR1ntP-(1–27).

The conformational changes in gp120, including the V3 loop, have been reported to be required for its interaction with a co-receptor after binding of gp120 to CD4 (21). The result of ELISA showed that GPR1ntP-(1–27) binds equally to rgp120 in the presence or absence of sCD4 (Fig. 7*C*), suggesting that GPR1ntP-(1–27) does not probably recognize the conformational changes in rgp120, especially in the V3 loop, induced by sCD4. This finding also suggested that the HIV-1 entry step at which gp120 interacts with a co-receptor after binding of envelope glycoprotein to CD4 is not a primary target for the anti-HIV-1 action of GPR1ntP-(1–27). Rather, we speculated that this peptide blocks an HIV-1 infection step before binding of gp120 to CD4 as described below.

It has also been reported that anti-V3 loop mAbs strongly bind to the intact virus particles, indicating that the V3 loop is already exposed on the surface of virions before interaction with CD4 receptor (52, 53). Indeed, we found that GPR1ntP-(1–27) binds to the highly purified virions (IIIB strain) even in the absence of sCD4 (Fig. 6), suggesting that GPR1ntP-(1–27) directly binds to the V3 loop exposed on the surface of intact HIV-1 virions under the physiological conditions. In contrast to the mAbs against the V3 loop, it has also been reported that none of four mAbs against the CD4-binding domain (CD4-bd) bind to intact virions, including IIIB strain, indicating that the CD4-bd is not exposed on the surface of intact virions (52).

It has been reported that there are CD4-dependent and CD4-independent sites for HIV-1 binding on the surface of $CD4^+$ cells (41). The presence of cell surface molecule(s) other than CD4 on MOLT-4 cells responsible for HIV-1 binding was also suggested by our data, *i.e.* detection of viral $p24^{Gag}$ bound to MOLT-4 cells even when the cells had been treated with anti-CD4 mAb before inoculation of virus (Fig. 8). In contrast to anti-CD4 mAb, anti-V3 loop mAb, heparin, and GPR1ntP-(1–27), expected to bind to the V3 loop exposed on the virions, almost completely inhibited the binding of HIV-1 to MOLT-4 cells (Fig. 8). Because CD4-bd on the surface of HIV-1 virions has not been reported to be exposed as described above, our results suggested that the binding of virus to the cells before interaction with CD4 is mediated by the V3 loop exposed on the surface of virions and that this initial CD4-independent virus binding step is an important target for GPR1ntP-(1–27) to inhibit HIV-1 infection.

Although GPR1 serves as a specific co-receptor for the HIV-1 variants, GPR1ntP-(1–27) blocked infection of diverse HIV-1 strains with different co-receptor usage. It may be explained in two ways. Firstly, the V3 loop is known to have the highest density of positively charged amino acids among all regions of gp120: it contains five to nine basic residues, and their distribution pattern within the V3 loop is well conserved among different strains (51, 55). Because GPR1ntP-(1–27) shows the highest ratio of acidic amino acids (net negative charge is −10) among the peptides used in this study (Table I), electrostatic interaction might be responsible for GPR1ntP-(1–27) to bind to basic residues within V3 loop, and to inhibit HIV-1 infection. Because the charge of amino acids in the V3 loop of R5 viruses is known to be more acidic than that of X4 or R5X4 viruses (51, 55), the relative resistance of R5 viruses (BaL and SF162) to GPR1ntP-(1–27) might be explained by the electrostatic repulsion between GPR1ntP-(1–27) and the V3 loop of the R5 viruses. Secondly, as the presence of a similarity in the conformation or antigenicity of the V3 loop has been suggested (52, 56), GPR1ntP-(1–27) would bind to this conserved conformation. Namely, an mAb, 447–52D, has been reported to bind to the V3 loop exposed on the surface of different HIV-1 strains even in the absence of the linear epitope (52, 56). Thus, recognition of the conserved conformation in the V3 loop by GPR1ntP-(1–27) might be important for its inhibitory activity to diverse HIV-1 strains.

The exact stoichiometry of GPR1ntP-(1–27) binding to target gp120 molecules in HIV-1 virions remains to be determined. It has been reported that gp120 is shed from infected cells and/or from virions soon after budding (57, 58). Schneider *et al.* (59) reported that virus-free culture fluid contains at least 100-fold more gp120 than virions pelleted from the same volume of culture supernatant. Thus, not only virion-associated gp120 but also free gp120 might also bind to GPR1ntP-(1–27) and affect its anti-HIV-1 activity.

Although GPR1ntP-(15–27) (YSYDLDYYSLESC) binds to rgp120 less efficiently than GPR1ntP-(1–27) (Fig. 7*F*), an inhibitory effect of GPR1ntP-(15–27) is much lower than GPR1ntP-(1–27) (Table III). Thus, there is a discrepancy between the binding ability to rgp120 and the anti-HIV-1 activity of GPR1ntP-(15–27). This is probably due to the inefficient binding of GPR1ntP-(15–27) to intact virions, because the conformation of monomer rgp120 is different from that of gp120 on the surface of HIV-1 virions. Namely, three gp120 molecules are associated noncovalently with the ectodomain of the gp41 envelope glycoprotein trimer to form oligomers (60).

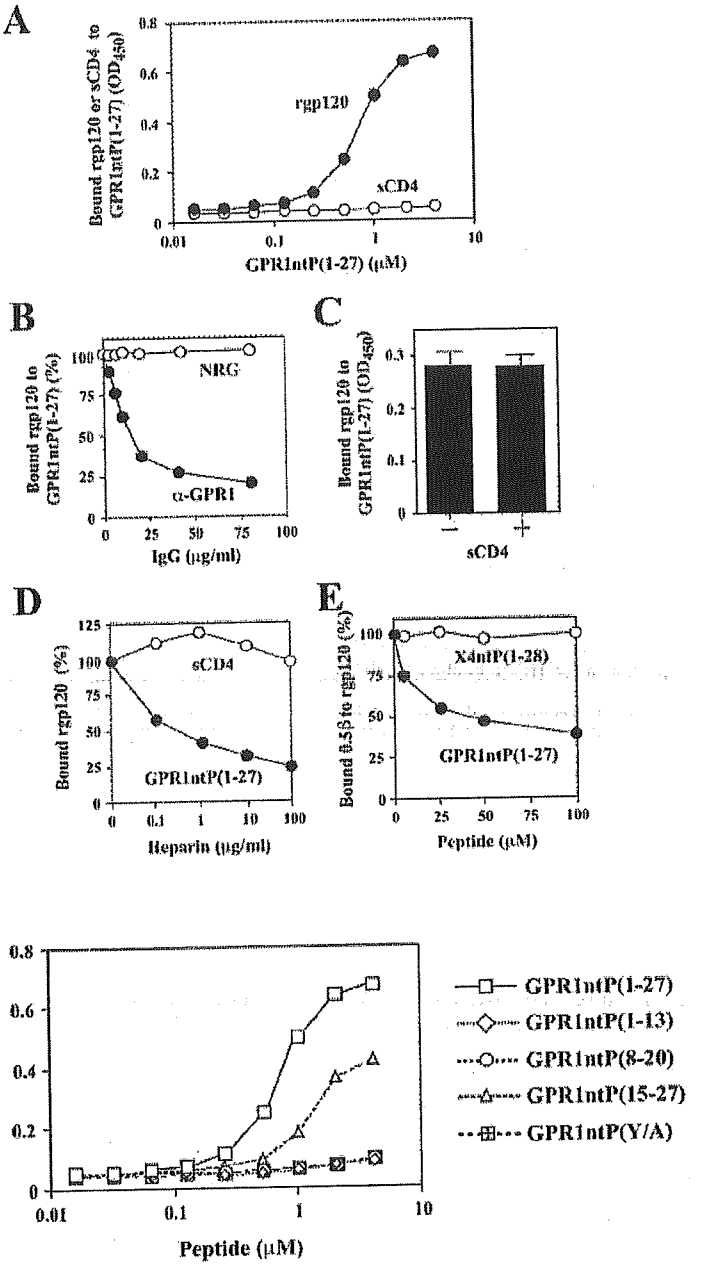

FIG. 7. **Specific interaction of GPR1ntP-(1–27) with rgp120 through its V3 loop.** *A*, binding of rgp120 or sCD4 to GPR1ntP-(1–27). Microtiter wells were coated with different concentrations of GPR1ntP-(1–27) (0.015–5 μM), and incubated with rgp120 (0.016 μM), or sCD4 (0.016 μM). Bound rgp120 and sCD4 were detected using the sera from AIDS patients and anti-sCD4 antibody, respectively, and shown as absorbance values at 450 nm (optical density at 450 nm (A_{450})). Each datum point is the mean of values obtained from triplicate samples, and experiment was repeated on at least three times. *B*, inhibition of rgp120 binding to GPR1ntP-(1–27) by α-GPR1 antibody. Microtiter wells were coated with GPR1ntP-(1–27) (1.0 μM), treated with α-GPR1 or normal rabbit IgG (NRG), and incubated with rgp120 (0.016 μM). Bound rgp120 was detected as described above. 100 and 0% binding correspond to OD_{450} values of 0.52 and 0.07, respectively. Data are the mean of values obtained from triplicate samples, and experiment was repeated on at least three times. *C*, effect of sCD4 on the binding of GPR1ntP-(1–27) to rgp120. Microtiter wells were coated with GPR1ntP-(1–27) (0.5 μM), then rgp120 (0.0016 μM), which had been incubated with or without sCD4 (0.016 μM) (37 °C, 1 h) was added, and bound rgp120 was detected as described above. Data are means and standard deviations from triplicate wells. *D*, inhibition of gp120-GPR1ntP-(1–27) interactions, but not that of gp120-sCD4 by heparin. Microtiter wells were coated with either GPR1ntP-(1–27) (1.0 μM) or sCD4 (0.016 μM), then rgp120 (0.016 μM) which had been incubated with or without heparin (37 °C, 1 h) was added, and bound rgp120 was detected as described above. 100 and 0% binding of rgp120 to GPR1ntP-(1–27) correspond to A_{450} values of 0.54 and 0.06, respectively. 100 and 0% binding of rgp120 to sCD4 correspond to A_{450} values of 0.65 and 0.09, respectively. Data are the mean of values obtained from triplicate samples, and experiment was repeated on at least three times. *E*, inhibition of the binding of V3 loop-specific, neutralizing mAb, 0.5β, to rgp120 by GPR1ntP-(1–27). Microtiter wells were coated with rgp120 (0.016 μM) and incubated with different concentrations of GPR1ntP-(1–27) or X4ntP-(1–28) (5–100 μM). Then 0.5β (ascites, 1:500 dilution) was added into each well, and the captured antibody was detected as described above. 100 and 0% binding of 0.5β to rgp120 correspond to A_{450} values of 0.36 and 0.05, respectively. Data are the mean values from triplicate samples, and three independent experiments gave similar results. *F*, binding of rgp120 to the fragment and mutant GPR1 peptides. Microtiter wells were coated with different concentrations of the peptides (0.015–5 μM), and incubated with rgp120 (0.016 μM). Bound rgp120 was detected using the sera from AIDS patients and shown as absorbance values at 450 nm. Data are the mean values from triplicate samples, and experiments were repeated three times to confirm results.

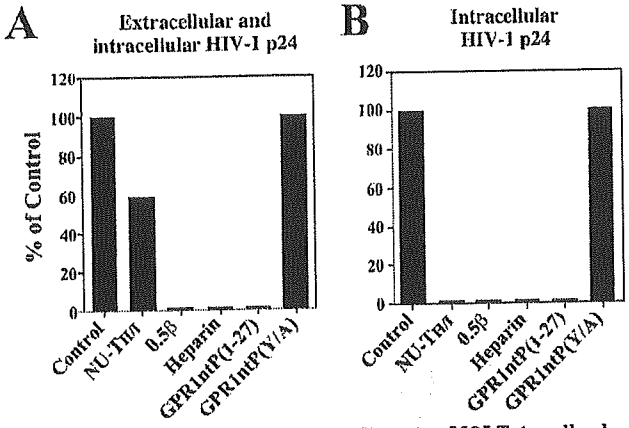

FIG. 8. **Inhibition of HIV-1 binding to MOLT-4 cells by GPR1ntP-(1–27).** *A*, detection of viral $p24^{Gag}$ associated with the cells, including both extracellular and intracellular portions after inoculation of HIV-1 (IIIB strain) to the cells. MOLT-4 cells were preincubated (1 h, 37 °C) with anti-CD4 mAb, NU-TH/I (10 μg/ml) before inoculation of HIV-1. HIV-1 was incubated (37 °C, 1 h) with anti-V3 loop mAb (0.5β, 10 μg/ml), heparin (10 μg/ml), GPR1ntP-(1–27) (20 μM), GPR1ntP-(Y/A) (20 μM), or control buffer before addition to the cells. After the cells were incubated with HIV-1 for 1 h at 37 °C, cell lysates were made to determine p24 core protein levels by ELISA. The control value for HIV-1 was 2840 pg of $p24^{Gag}$ per 10^7 cells. *B*, detection of viral $p24^{Gag}$ present in the intracellular portion after HIV-1 binding to MOLT-4 cells. After MOLT-4 cells were incubated with HIV-1 for 1 h at 37 °C, the cells were treated with trypsin to remove viral particles still attached to the cell surface. The control value for HIV-1 was 1670 pg of $p24^{Gag}$ per 10^7 cells. Under these experimental conditions, normal mouse IgG1 with the same isotype as NU-TH/I and 0.5β had no effect at 10 μg/ml. Data are the mean values from triplicate samples, and experiments were repeated three times to confirm results.

In this study, we showed that the mutant peptide (GPR1ntP-(Y/A)) substituting tyrosine to alanine does not inhibit HIV-1 infection (Table III) and has no activity for binding to rgp120 (Fig. 7*F*). Thus, tyrosine residues in GPR1ntP-(1–27) could contribute for interaction with rgp120 and play a crucial role in inhibition of HIV-1 infection. Farzan *et al.* (61) have shown that tyrosine residues from NH_2-ECR of CCR5 contribute to the co-receptor activity through their sulfation, a post-translational modification resulting in the addition of a negatively charged sulfate. Although the sulfation of tyrosine residues in NH_2-ECR of GPR1 remains to be elucidated, it is possible that the introduction of sulfated tyrosine residue to GPR1ntP-(1–27) will enhance its anti-HIV-1 activity as a result of an addition of negative charge to GPR1ntP-(1–27). With regard to GPR1ntP-(1–27) analogs, we previously reported that a hexapeptide derived from GPR1ntP-(1–27) (amino acid residues from 17 to 22: YDLDYY) has a weak anti-HIV-1 activity at concentrations around 500 μM (62). The introduction of sulfation to tyrosine residues of this hexapeptide, however, did not significantly improve its inhibitory activity as compared with a nonsulfated hexapeptide (62). Because GPR1ntP-(15–27) binds to rgp120 less efficiently than GPR1ntP-(1–27), the amino acid residues of GPR1ntP-(1–27) from 1 to 14 (MEDLEETL-FEEFEN), which contain no tyrosine but several acidic amino acids, will also be necessary for the strong inhibitory activity of GPR1ntP-(1–27) against HIV-1 infection. Thus, the addition of acidic amino acid residues to sulfated tyrosine may be important to develop GPR1ntP-(1–27) analogs with enhanced anti-HIV-1 activities. This possibility is currently under investigation.

The entry stages, including initial attachment in HIV-1 replication cycle, are effective targets for the development of new antiretroviral therapies, because *de novo* infection of HIV-1 to humans can be prevented. This has already been shown by the clinical application of several antiretroviral agents. For instance, PRO 542 is a fusion protein of the gp120-binding domain of CD4 with immunoglobulin constant domains, and is expected to block the interaction between gp120 and the CD4 receptor (63); or T20 is a peptide (36 amino acids) that inhibits the HIV-1 fusion step through binding to the viral envelope protein gp41 (64, 65). With a view to the antiviral potency of GPR1ntP-(1–27), the direct use of this peptide as a therapeutic agent will remain uncertain until studies of toxicity and pharmacokinetics are carried out. A critical concern with peptide-based antiviral therapy is its potential to elicit an antibody response to a peptide and make it ineffective (66). Because the amino acid sequence of GPR1ntP-(1–27) is derived from human, the antigenicity of GPR1ntP-(1–27) may be little or not at all in treated patients. The elucidation of the *in vitro* antiviral mechanism of GPR1ntP-(1–27) shown in this study will disclose valuable insights in the development of a new class of GPCR-based and peptide-based HIV-1 inhibitors.

Acknowledgments—We thank T. Nakamura for excellent technical assistance. We are grateful to Drs. T. Kumanishi (Niigata University, Niigata, Japan) and S. Matsushita (Kumamoto University, Kumamoto, Japan) for kindly providing us with NP-2 glioma cells and an anti-V3 loop MAb, 0.5β, respectively. We also thank Dr. H. Holmes (AIDS Reagent Project of the United Kingdom Medical Research Council) for supplying rgp120, sCD4, and anti-sCD4 antibody.

REFERENCES

1. Barre-Sinoussi, F., Chermann, J. C., Rey, F., Nugeyre, M. T., Chamaret, S., Gruest, J., Dauguet, C., Axler-Blin, C., Vezinet-Brun, F., Rouzioux, C., Rozenbaum, W., and Montagnier, L. (1983) *Science* **220,** 868–871
2. Gallo, R. C., Salahuddin, S. Z., Popovic, M., Shearer, G. M., Kaplan, M., Haynes, B. F., Palker, T. J., Redfield, R., Oleske, J., Safai, B., White, G., Foster, P., and Markham, P. D. (1984) *Science* **224,** 500–503
3. D'Souza, M. P., and Harden, V. A. (1996) *Nat. Med.* **12,** 1293–1300
4. Alkhatib, G., Combadiere, C., Broder, C. C., Feng, Y., Kennedy, P. E., Murphy, P. M., and Berger, E. A. (1996) *Science* **272,** 1955–1958
5. Choe, H., Farzan, M., Sun, Y., Sullivan, N., Rollins, B., Ponath, P. D., Wu, L., Mackay, C. R., LaRosa, G., Newman, W., Gerard, N., Gerard, C., and Sodroski, J. (1996) *Cell* **85,** 1135–1148
6. Deng, H., Liu, R., Ellmeier, W., Choe, S., Unutmaz, D., Burkhart, M., Di Marzio, P., Marmon, S., Sutton, R. E., Hill, C. M., Davis, C. B., Peiper, S. C., Schall, T. J., Littman, D. R., and Landau, N. R. (1996) *Nature* **381,** 661–666
7. Doranz, B. J., Rucker, J., Yi, Y., Smyth, R. J., Samson, M., Peiper, S. C., Parmentier, M., Collman, R. G., and Doms, R. W. (1996) *Cell* **85,** 1149–1158
8. Dragic, T., Litwin, V., Allaway, G. P., Martin, S. R., Huang, Y., Nagashima, K. A., Cayanan, C., Maddon, P. J., Koup, R. A., Moore, J. P., and Paxton, W. A. (1996) *Nature* **381,** 667–673
9. Feng, Y., Broder, C. C., Kennedy, P. E., and Berger, E. A. (1996) *Science.* **272,** 872–877
10. Takeuchi, Y., Akutsu, M., Murayama, K., Shimizu, N., and Hoshino, H. (1991) *J. Virol.* **65,** 1710–1718
11. Shimizu, N., Kobayashi, M., Liu, H. Y., Kido, H., and Hoshino, H. (1995) *FEBS Lett.* **358,** 48–52
12. Shimizu, N. S., Shimizu, N. G., Takeuchi, Y., and Hoshino, H. (1994) *J. Virol.* **68,** 6130–6135
13. Shimizu, N., Soda, Y., Kanbe, K., Liu, H. Y., Jinno, A., Kitamura, T., and Hoshino, H. (1999) *J. Virol.* **73,** 5231–5239
14. Shimizu, N., Soda, Y., Kanbe, K., Liu, H. Y., Mukai, R., Kitamura, T., and Hoshino, H. (2000) *J. Virol.* **74,** 619–626
15. Liu, H. Y., Soda, Y., Shimizu, N., Haraguchi, Y., Jinno, A., Takeuchi, Y., and Hoshino, H. (2000) *Virology* **278,** 276–288
16. Dragic, T., Trkola, A., Lin, S. W., Nagashima, K. A., Kajumo, F., Zhao, L., Olson, W. C., Wu, L., Mackay, C. R., Allaway, G. P., Sakmar, T. P., Moore, J. P., and Maddon, P. J. (1998) *J. Virol.* **72,** 279–285
17. Rabut, G. E., Konner, J. A., Kajumo, F., Moore, J. P., and Dragic, T. (1998) *J. Virol.* **72,** 3464–3468
18. Doranz, B. J., Orsini, M. J., Turner, J. D., Hoffman, T. L., Berson, J. F., Hoxie, J. A., Peiper, S. C., Brass, L. F., and Doms, R. W. (1999) *J. Virol.* **73,** 2752–2761
19. Genoud, S., Kajumo, F., Guo, Y., Thompson, D., and Dragic, T. (1999) *J. Virol.* **73,** 1645–1648
20. Brelot, A., Heveker, N., Montes, M., and Alizon, M. (2000) *J. Biol. Chem.* **275,** 23736–23744
21. Dragic, T. (2001) *J. Gen. Virol.* **82,** 1807–1814
22. Jinno, A., Shimizu, N., Soda, Y., Haraguchi, Y., Kitamura, T., and Hoshino, H. (1998) *Biochem. Biophys. Res. Commun.* **243,** 497–502
23. Soda, Y., Shimizu, N., Jinno, A., Liu, H. Y., Kanbe, K., Kitamura, T., and Hoshino, H. (1999) *Biochem. Biophys. Res. Commun.* **258,** 313–321
24. Salahuddin, S. Z., Markham, P. D., Wong-Staal, F., Franchini, G., Kalyanaraman, V. S., and Gallo, R. C. (1983) *Virology* **129,** 51–64
25. Srivastava, B. I., and Minowada, J. (1983) *Leuk. Res.* **7,** 331–338
26. Nagumo, T., and Hoshino, H. (1988) *Jpn. J. Cancer Res.* **79,** 9–11
27. Takeuchi, Y., Inagaki, M., Kobayashi, N., and Hoshino, H. (1987) *Jpn. J. Cancer Res.* **78,** 11–15

28. Popovic, M., Sarngadharan, M. G., Read, E., and Gallo, R. C. (1984) *Science* **224,** 497–500
29. Gartner, S., Markovits, P., Markovitz, D. M., Kaplan, M. H., Gallo, R. C., and Popovic, M. (1986) *Science* **233,** 215–219
30. Simmons, G., Wilkinson, D., Reeves, J. D., Dittmar, M. T., Beddows, S., Weber, J., Carnegie, G., Desselberger U., Gray, P. W., Weiss, R. A., and Clapham, P. R. (1996) *J. Virol.* **70,** 8355–8360
31. Matsushita, S., Robert-Guroff, M., Rusche, J., Koito, A., Hattori, T., Hoshino, H., Javaherian, K., Takatsuki, K., and Putney, S. (1988) *J. Virol.* **62,** 2107–2114
32. Oravecz, T., and Norcross, M. A. (1993) in *Leukocyte Typing V: White Cell Differentiation Antigens* (Schlossman, S. F., *et al.*, eds) pp. 476–478, Oxford University Press, Oxford
33. Chesebro, B., and Wehrly, K. (1988) *J. Virol.* **62,** 3779–3788
34. Pincus, S. H., Wehrly, K., and Chesebro, B. (1991) *BioTechniques* **10,** 336–342
35. Frumkin, L. R., Patterson, B. K., Leverenz, J. B., Agy, M. B., Wolinsky, S. M., Morton, W. R., and Corey, L. (1995) *J. Gen. Virol.* **76,** 2467–2476
36. Kozak, S. L., Platt, E. J., Madani, N., Ferro, F. E., Jr., Peden, K., and Kabat, D. (1997) *J. Virol.* **71,** 873–882
37. Platt, E. J., Wehrly, K., Kuhmann, S. E., Chesebro, B., and Kabat, D. (1998) *J. Virol.* **72,** 2855–2864
38. Mckeating, J. (1995) in *The Practical Approach Series, HIV Volume 1* (Karn, J., ed) pp. 117–126, Oxford University Press, New York
39. Quiros, E., Garcia, F., Maroto, M. C., Bernal, M. C., Cabezas, T., and Piedrola, G. (1995) *J. Med. Microbiol.* **42,** 411–414
40. Saiki, R. K., Gelfand, D. H., Stoffel, S., Scharf, S. J., Higuchi, R., Horn, G. T., Mullis, K. B., and Erlich H. A. (1988) *Science* **239,** 487–491
41. Valenzuela, A., Blanco, J., Krust, B., Franco, R., and Hovanessian, A. G. (1997) *J. Virol.* **71,** 8289–8298
42. Clapham, P. R., Blanc, D., and Weiss, R. A. (1991) *Virology* **181,** 703–715
43. Bess, J. W., Jr., Powell, P. J., Issaq, H. J., Schumack, L. J., Grimes, M. K., Henderson, L. E., and Arthur, L. O. (1992) *J. Virol.* **66,** 840–847
44. Dettenhofer, M., and Yu, X.-F. (1999) *J. Virol.* **73,** 1460–1467
45. Van Opstal, O., Fabry, L., Francotte, M., Thiriart, C., and Bruck, C. (1995) in *The Practical Approach Series, HIV Volume 2* (Karn, J., ed) pp. 105–122, Oxford University Press, New York
46. Cormier, E. G., Persuh, M., Thompson, D. A. D., Lin, S. W., Sakmer, T. P., Olson, W. C., and Dragic, T. (2000) *Proc. Natl. Acad. Sci. U. S. A.* **97,** 5762–5767
47. Farzan, M., Vasilieva, N., Schnitzler, C. E., Chung, S., Robinson, J., Gerard, N. P., Gerard, C., Choe, H., and Sodroski, J. (2000) *J. Biol. Chem.* **275,** 33516–33521
48. Batinic, D., and Robey, F. A. (1992) *J. Biol. Chem.* **267,** 6664–6671
49. Rider, C. C., Coombe, D. R., Harrop, H. A., Hounsell, E. F., Bauer, C., Feeney, J., Mulloy, B., Mahmood, N., Hay, A., and Parish, C. R. (1994) *Biochemistry* **33,** 6974–6980
50. Harrop, H. A., and Rider, C. C. (1998) *Glycobiology* **8,** 131–137
51. Moulard, M., Lortat-Jacob, H., Mondor, I., Roca, G., Wyatt, R., Sodroski, J., Zhao, L., Olson, W., Kwong, P. D., and Sattentau, Q. J. (2000) *J. Virol.* **74,** 1948–1960
52. Nyambi, P. N., Gorny, M. K., Bastiani, L., van der Groen, G., Williams, C., and Zolla-Pazner, S. (1998) *J. Virol.* **72,** 9384–9391
53. Gorny, M. K., Revesz, K., Williams, C., Volsky, B., Louder, M. K., Anyangwe, C. A., Krachmarov, C., Kayman, S. C., Pinter, A., Nadas, A., Nyambi, P. N., Mascola, J. R., and Zolla-Pazner, S. (2004) *J. Virol.* **78,** 2394–2404
54. Skinner, M. A., Langlois, A. J., McDanal, C. B., McDougal, J. S., Bolognesi, D. P., and Matthews, T. J. (1988) *J. Virol.* **62,** 4195–4200
55. Hwang, S. S., Boyle, T. J., Lyerly, H. K., and Cullen, B. R. (1991), *Science* **253,** 71–74
56. Cecilia, D., Vineet, N., KewalRamani, O'Leary, J., Volsky, B., Nyambi, P., Burda, S., Xu, S., Littman, D R., and Zolla-Pazner, S. (1998) *J. Virol. 1998* **72,** 6988–6996
57. Layne, S. P., Merges M. J., Dembo, M., Spouge, J. L., Conley S. R., Moore J. P., Raina, J. L., Renz, H., Gelderblom, H. R., and Nara, P. L. (1992), *Virology* **189,** 695–714
58. Hart, T. K., Klinkner, A. M., Ventre J., and Bugelski, P. J. (1993) *J. Histochem. Cytochem.* **41,** 265–271
59. Schneider, J., Kaaden, O., Copeland, T. D., Oroszlan, S., and Hunsmann, G. (1986) *J. Gen. Virol.* **67,** 2533–2538
60. Hunter, E. (1997) in *Retroviruses* (Coffin, J. M., Hughes, S. H., and Varmus, H. E., eds) pp. 71–120, Cold Spring Harbor Laboratory Press, Cold Spring Harbor, NY
61. Farzan, M., Mirzabekov, T., Kolchinsky, P., Wyatt, R., Cayabyab, M., Gerard, N. P., Gerard, C., Sodroski, J., and Choe, H. (1999) *Cell* **96,** 667–676
62. Ikeda, K., Konishi, K., Saito, M., Hoshino, H., and Tanaka, K. (2001) *Bioorg. Med. Chem. Lett.* **11,** 2607–2609
63. Jacobson, J. M., Lowy, I., Fletcher, C. V., O'Neill, T. J., Tran, D. N., Ketas, T. J., Trkola, A., Klotman, M. E., Maddon, P. J., Olson, W. C., and Israel, R. J. (2000) *J. Infect. Dis.* **182,** 326–329
64. Kilby, J. M., Hopkins, S., Venetta, T. M., DiMassimo, B., Cloud, G. A., Lee, J. Y., Alldredge, L., Hunter, E., Lambert, D., Bolognesi, D., Matthews, T., Johnson, M. R., Nowak, M. A., Shaw, G. M., and Saag, M. S. (1998) *Nat. Med.* **4,** 1302–1307
65. Munoz-Barroso, I., Durell, S., Sakaguchi, K., Appella, E., and Blumenthal, R. (1998) *J. Cell Biol.* **140,** 315–323
66. LaBranche, C. C., Galasso, G., Moore, J. P., Bolognesi, D. P., Hirsch, M. S., and Hammer, S. M. (2001) *Antiviral Res.* **50,** 95–115

Available online at www.sciencedirect.com
SCIENCE DIRECT
Microbes and Infection 7 (2005) 29–40
Microbes and Infection
www.elsevier.com/locate/micinf

Original article

Efficient formation of vesicular stomatitis virus pseudotypes bearing the native forms of hepatitis C virus envelope proteins detected after sonication

Kazushi Tamura [a,b], Atsushi Oue [a], Atsushi Tanaka [a], Nobuaki Shimizu [a], Hitoshi Takagi [c], Nobuyuki Kato [d], Akihiro Morikawa [b], Hiroo Hoshino [a,*]

[a] *Department of Virology and Preventive Medicine, Gunma University Graduate School of Medicine, 3-39-22 Showa-machi, Maebashi, Gunma 371-8511, Japan*
[b] *Department of Pediatrics and Developmental Medicine, Gunma University Graduate School of Medicine, 3-39-22 Showa-machi, Maebashi, Gunma 371-8511, Japan*
[c] *Department of Medicine and Molecular Science, Gunma University Graduate School of Medicine, 3-39-22 Showa-machi, Maebashi, Gunma 371-8511, Japan*
[d] *Department of Molecular Biology, Institute of Cellular and Molecular Biology, Okayama University Graduate School of Medicine and Dentistry, Okayama 700-8558, Japan*

Received 17 May 2004; accepted 15 September 2004

Available online 09 December 2004

Abstract

Hepatitis C virus (HCV) causes chronic hepatitis, liver cirrhosis and hepatocellular carcinoma in addition to acute hepatitis. The HCV genome encodes two envelope glycoproteins, E1 and E2. To investigate the role of E1 and E2 in HCV infection, we used a recombinant vesicular stomatitis virus (VSV), VSVΔG*, harboring the green fluorescent protein gene instead of the VSV G envelope protein gene. It was complemented with the native form of E1 and E2, or E1 or E2 alone, to make HCV pseudotypes VSVΔG*(HCV), VSVΔG*(E1), and VSVΔG*(E2). Neither E1 nor E2 expression was detected on the cell surface, as reported. Unlike previous reports, infectious activities of VSVΔG*(HCV), VSVΔG*(E1) and VSVΔG*(E2) pseudotypes were detected under conditions where VSV was completely neutralized by anti-VSV. We could enhance the infectious titers 100-fold by sonication upon virus harvest. Bovine lactoferrin efficiently inhibited infection by VSVΔG*(HCV) as well as VSVΔG*(E2), as the interaction between E2 and lactoferrin has been thought to contribute to the inhibition of HCV infectivity. VSVΔG*(HCV) infected many adherent cell lines, including hepatic cell lines, but not most hematopoietic cell lines. Treatment of cells with trypsin, tunicamycin, or sulfated polysaccharides before infection reduced the infectivity of VSVΔG*(HCV) by about 90%, suggesting that a cell surface protein(s) with sugar chains plays an important role in HCV infection. The VSV pseudotypes developed here would be useful for analyzing the early stages of HCV infection.

Keywords: HCV; Pseudotype; Envelope; Sonication; Glycosylation

1. Introduction

Hepatitis C virus (HCV) has been one of the major causative agents of posttransfusion and sporadic hepatitis [1]. At present, transfusion-associated hepatitis C has been virtually eliminated in developed countries, and risk factors that most are strongly correlated with HCV infection there are illegal drug use and high-risk sexual behavior. Current worldwide estimations suggest that more than 200 million people are infected with HCV [2]. The infection frequently develops into chronic hepatitis, which further leads to the development of liver cirrhosis and hepatocellular carcinoma [3,4]. The mechanisms involved in HCV infection and HCV-mediated disease progression are not well understood, and a therapy effective for most HCV-infected patients is not yet available.

HCV is an enveloped, positive-stranded RNA virus belonging to the Flaviviridae family [2]. The viral genome contains

* Corresponding author. Tel.: +81 27 220 8000; fax: +81 27 220 8006.
E-mail address: hoshino@med.gunma-u.ac.jp (H. Hoshino).

1286-4579/$ - see front matter © 2004 Published by Elsevier SAS.
doi:10.1016/j.micinf.2004.09.006

a single open-reading frame of approximately 9.5 kb that codes for a large polyprotein precursor of 3000 amino acids (aa) [5,6] (Fig. 1a). Structural proteins are located in the N-terminal of the precursor polyprotein, which is to be cleaved by cellular signal peptidases. The core protein (C) is followed by two putative envelope proteins, E1 and E2. A small protein, p7, is produced by the cleavage of the E2 protein. Downstream of the structural proteins, non-structural proteins (NS2, NS3, NS4A, NS4B, NS5A, and NS5B) are located [7,8]. The E1 and E2 envelope proteins form a non-covalently linked heterodimer, which probably represents the native pre-budding complex, in the endoplasmic reticulum (ER) [9].

The binding of the virus to the host cell surface receptor(s) is the first step in the infection process. As in most enveloped viruses, E1 and E2 are believed to be the major viral attachment proteins in HCV. There has been no clear evidence as to which protein, E1 or E2, defines the interaction with human cells, because of the lack of a suitable experimental system for HCV entry. It has been reported that a truncated, soluble form of E2 binds to human CD81 (hCD81) and human scavenger receptor class B type I (SR-IB), suggesting that

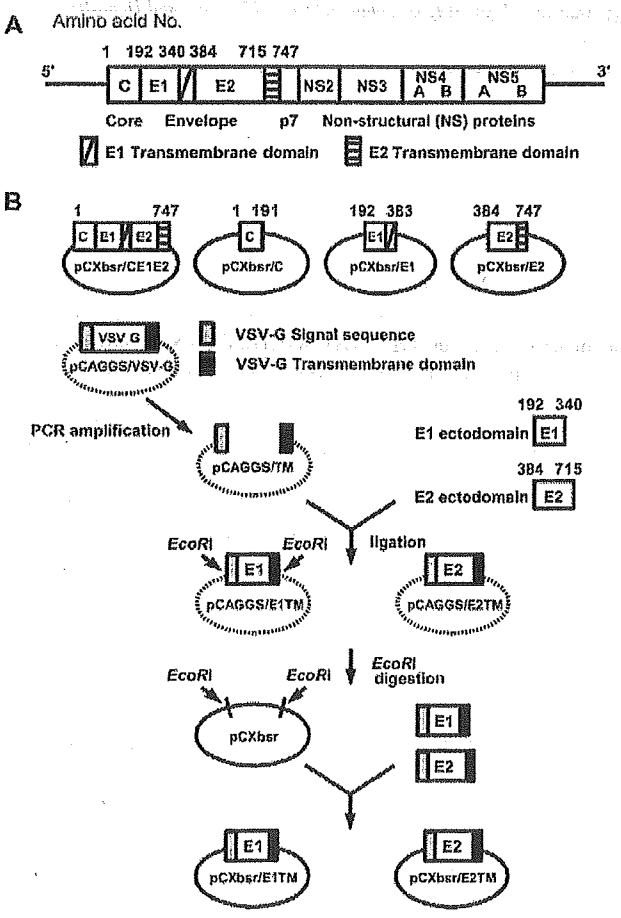

Fig. 1. Preparation of plasmids expressing HCV envelope proteins. (a) Structure of HCV genome. (b) Schematic representation of the plasmids and the chimeric gene constructs for the expression of HCV envelope glycoproteins. TM represents the signal sequence and the transmembrane domain of VSV G protein.

hCD81 or SR-IB is a candidate cellular receptor for HCV [10,11]. Furthermore, HCV particles have also been reported to utilize the LDL receptor for binding and their entry into the cells [12,13]. But it is still unknown whether they serve as functional receptors, since the expression of neither hCD81 nor the LDL receptor is restricted in hepatocytes, and hCD81 transgenic mice are resistant to HCV infection [14]. There may also be a functional difference between the native form of HCV envelope protein and the soluble form of E2. The main obstacle to clarifying these points is the lack of suitable tools with which to evaluate the attachment to and entry into the target cells quantitatively. Recently, to analyze virus entry mediated by HCV envelopes, systems for the production of vesicular stomatitis virus (VSV) pseudotypes bearing modified HCV envelope proteins have been reported [15–17]. To express the HCV envelope proteins on the cell surface to incorporate them into VSV virions, chimeric HCV E1 and E2 proteins containing the transmembrane domain and cytoplasmic tail of VSV G glycoprotein (VSV G) were generated. Otherwise, E1 or E2 is not expressed on the cell surface. There is the possibility that these pseudotypes may show a different infectivity from the viruses bearing the native forms of HCV envelopes.

In this study, we developed a system to prepare VSV pseudotypes expected to bear the native HCV envelope proteins, E1E2, E1 or E2. That is, cells were transfected with the native structural protein genes, and then infected with a recombinant VSV, VSVΔG*G, containing the green fluorescent protein (GFP) gene as a reporter instead of VSV G [18]. Unlike previous reports [15–17], we could detect pseudotype virus activities after transfection of not only the native structural protein gene C–E1–E2, but also the unmodified E1 or E2 gene. These pseudotype virus-like activities were not neutralized by any sera from chronic hepatitis C patients, as previously reported using pseudotypes with chimeric HCV envelopes [17,19]. These infectious activities were inhibited by treatment with bovine lactoferrin, as we reported using PCR for detection of HCV infection [20,21]. Using these new VSV pseudotypes, we further examined the mechanism involved in HCV infection. That is, the infectivity of pseudotype viruses was studied in various cell lines, and the effects of chemical reagents on the infection were tested.

2. Materials and methods

2.1. Cells

293T is derived from the human embryonic kidney cell line 293 and contains the SV40 large T-antigen [22]. The other cell lines used in this study and their derivations are listed in Table 3. BALL-1, C8166, C91/PL, Daudi, HEL, HL-60, K562, Molt-4, MT-2, Raji, TALL-1, U937 and Wil2NS were cultured in RPMI-1640 medium (Nissui, Tokyo, Japan) supplemented with 10% fetal calf serum (FCS). 293T, A172, HepG2, HOS and Huh7 were maintained in Dulbecco's modi-

fied Eagle's medium (DMEM; Nissui) supplemented with 10% FCS. U87MG was maintained in DMEM supplemented with 20% FCS. HUK-1, NP2 and U251 were maintained in Eagle's medium (Nissui) supplemented with 10% FCS. The maintenance of PH5CH8 cells was previously described in detail [23]. Human brain microvascular endothelial cells (HBMECs, Applied Cell Biology Research Institute, WA) were maintained in endothelial cell basal medium 2 supplemented with EGM-2 additives (Clontecs, CA). Human brain pericytes (HBP) were derived from surgically dissected human brain tissue. HBP cells were maintained in RPMI-1640 medium supplemented with 10% FCS, 10 μg/ml of endothelial cell growth supplement, and 10 ng/ml of epidermal growth factor. All culture media were supplemented with 50 μg/ml of kanamycin before use.

2.2. Plasmids

Fragments of the HCV C, E1 and E2 genes were obtained from a subclone of an infectious clone of HCV, subtype Ib [6], the predominant subtype in Japan, and cloned into pCXbsr, a Moloney murine leukemia virus-based retroviral vector plasmid [24]. Mammalian expression plasmids encoding HCV core protein (pCXbsr/C), HCV E1 protein (pCXbsr/E1), HCV E2 protein (pCXbsr/E2) and all HCV structural proteins, core-E1–E2 (pCXbsr/CE1E2), were made as shown in Fig. 1b. To construct retroviral expression plasmids encoding chimeric HCV envelope proteins, we generated the plasmid pCAGGS/TM, encoding the signal sequence, the transmembrane domain, and the cytoplasmic tail of the VSV G protein, as described below. pCAGGS/TM was amplified by PCR using pCAGGS/VSV-G [25] as a template, in which VSV (Indiana serotype) G protein was placed under control of the CAG promoter, and the following primers:

- sense primer, 5′-AAAAGCTCTATTGCCTCTTTTT-TCTTTATC;
- antisense primer, 5′-GCAATTCACCCCAATGAATA-AAAAGGCTAA.

The coding sequence for the ectodomain of HCV E1 (aa 192–340) was amplified by PCR using pCXbsr/CE1E2 as a template and the following primers:

- sense primer, 5′-TATGAAGTGCGCAACGTGTCCGG-GGTGTAC;
- antisense primer, 5′-GATCCGGAGCAACTGCGA-TACCACCAGGGC.

The ectodomain of the HCV E2 (aa 384–715) genomic region was amplified by PCR using pCXbsr/CE1E2 as a template and the following primers:

- sense primer, 5′-GCTACCTACACGTCAGGGGGGAC-GGTAGGC;
- antisense primer, 5′-TCTGATTACAACGGAGACAAC-CACTGACCC.

The ectodomains of E1 and E2 sequences were subcloned into pCAGGS/TM, using a Blunting High kit (Toyobo, Tokyo, Japan), and the plasmids pCAGGS/E1TM and pCAGGS/E2TM were isolated. pCAGGS/E1TM and pCAGGS/E2TM digested with *Eco*RI (Takara, Siga, Japan) were subcloned into pCXbsr, resulting in the formation of pCXbsr/E1TM and pCXbsr/E2TM, respectively (Fig. 1b).

2.3. Immunofluorescence staining of E1 and E2

293T cells were seeded onto slide glasses and the next day transfected with the expression plasmid vectors for HCV envelope proteins using FuGENE6 (Roche, Basel, Switzerland). After 32 h, the cells were tested for the expression of the viral envelope proteins by indirect immunofluorescence. Namely, the cells were washed with phosphate-buffered saline (PBS) and fixed with 4% paraformaldehyde in PBS for 5 min at room temperature. Half the fixed cell samples were then permeabilized with 0.1% Triton X-100 for 5 min at room temperature. A mouse monoclonal antibody (MAb) to E1, E1-384 [26], and a rat MAb to E2, Mo-12 [27], were used as follows. The MAb diluted to 1:1000 in PBS was added as the primary antibody and incubated for 60 min at 37 °C. After a wash with PBS, fluorescein isothiocyanate (FITC)-conjugated rat anti-mouse IgG or FITC-conjugated rabbit anti-rat IgG (Dako, Glostrup, Denmark) diluted 1:50 in PBS was added, and the cells were incubated for 60 min at 37 °C. After three washes in PBS, the cells seeded on slide glasses were embedded with a solution of glycerol in PBS and examined with a fluorescence microscope for the expression of HCV glycoproteins.

2.4. Preparation of pseudotype viruses

VSVΔG*G is the recombinant VSV, generated by reverse genetics, as described previously [18] and kindly provided by Dr. M.A. Whitt. To generate VSV pseudotype viruses, 2×10^6 293T cells were grown in a poly-L-lysine-coated 60-mm dish and transfected with plasmids. Thirty-two hours after transfection, the cells were infected with VSVΔG*G at an MOI of 2 for 2.5 h at 37 °C in a 5% CO_2 incubator. Virus-infected cells were washed with serum-free DMEM and incubated in 1 ml of goat anti-VSV polyclonal antibody (diluted at 1:10) for 40 min at 37 °C to neutralize unabsorbed virus. This concentration was enough to completely neutralize the undiluted VSVΔG*G. Then, they were again washed with serum-free DMEM four times, and culture medium was added. After 15 h of incubation at 37 °C, the culture supernatants + adherent cells were harvested and centrifuged at 350 × *g* for 3 min at room temperature. Then, cell pellets were either sonicated or left untreated, and the virus samples were clarified by centrifugation at 350 × *g* for 5 min at room temperature to remove cell debris. Virus samples were stock frozen at –80 °C. These samples were found to show compatible properties with those of HCV virions, as described in Table 2. As control pseudotypes, VSVΔG*G and VSVΔG* were used. VSVΔG*G was prepared by infecting 293T cells that had been transfected with pCAGGS/VSV-G, while the VSVΔG* sample was prepared by infecting 293T cells that had been transfected with pCXbsr plasmid containing no envelope protein.

2.5. Detection of HCV envelope proteins and VSV structural proteins in pseudotype virus samples by Western blotting

We prepared 293T cells transfected with the expression plasmid vectors for HCV envelope proteins described in Table 2. These cells were infected with VSVΔG*G. We also prepared the 293T cells transfected with the expression plasmid vectors for HCV envelopes that were not infected with VSVΔG*G. These samples were sonicated and centrifuged at 350 × *g* for 5 min. Each 3-ml supernatant was subjected to ultracentrifugation (27,000 rpm for 3 h at 4 °C) through 2 ml of a 20% sucrose layer using an SCP70H HITACHI. Pellets were suspended in 30 μl of sample buffer (1% SDS, 1% 2-mercaptomethanol, 50 mM Tris–HCl [pH 6.8], and 20% glycerol). The samples were loaded onto 10% SDS-PAGE gel. E1 proteins were detected using an anti-E1 mouse MAb, E1-384 [26] (diluted at 1:1000), and then HRP-conjugated anti-mouse IgG (Dako; diluted at 1:1000). E2 proteins were detected using an anti-E2 rat MAb, Mo-12 [27] (diluted at 1:1000), and HRP-conjugated anti-rat IgG (Dako). VSV structural proteins were detected using goat anti-VSV polyclonal antibody (diluted at 1:4000), and HRP-conjugated anti-goat IgG (Dako). HRP-conjugated antibodies bound to filters were detected using enhanced chemiluminescence.

2.6. Titration of pseudotype viruses using various cell lines

Cells (2×10^4) were seeded into wells of 96-well flat-bottom plates. After 36 h of incubation, the cells were infected with the virus samples defined in Table 2 and incubated at 37 °C for 24 h. The HepG2 cell line was incubated at 33 °C, because a lower temperature had a better effect on infection in this cell line. Infectious units (IU) of the samples were determined by counting the number of GFP-expressing cells under a fluorescence microscope.

2.7. Sonication for preparation of pseudotype virus samples

As the native form of the HCV envelope protein was reported not to be expressed on the cell surface [28,29], we tested a sonication step to efficiently recover HCV pseudotypes. For this, the VSV pseudotype samples harvested as described above were sonicated with a SONIFIER 250 (Branson, CT) for 0.2 s five times on ice. The samples were centrifuged at 350 × *g* for 5 min, and supernatants were aliquoted and stocked frozen at −80 °C. HepG2 cells were used for titration of the pseudotype samples prepared with or without sonication. After 24 h of infection, IU were determined as described above.

2.8. Neutralization of the pseudotype virus samples

To judge whether the infectivity of each virus sample was HCV- or VSV-specific, the pseudotype virus samples were incubated with serially diluted polyclonal antibody against VSV in the presence or absence of human sera from patients with chronic HCV infection (final concentration up to 20%) for 30 min at 37 °C, and HepG2 cells were infected with these samples. After 24 h of incubation, the amount of remaining infectious titer was determined as described above. All previous reports have, however, shown that sera from patients with chronic HCV infection hardly neutralized chimeric E1 or E2 pseudotypes [17,19].

2.9. Treatment of the pseudotype viruses with chemicals

Pseudotype virus samples expected to bear E1, E2 or E1E2 protein were preincubated with various concentrations of bovine lactoferrin (Wako, Tokyo, Japan) at 37 °C for 1 h and inoculated onto HepG2 cells. After 1.5 h of incubation, the cells were washed with DMEM three times and incubated with fresh culture medium. The VSVΔG*(HCV) pseudotype was preincubated with heparin (Wako), dextran sulfate (molecular weight (MW) 8000 or 500,000) or dextran (MW 7000; Sigma, MO) at 37 °C for 1 h, and HepG2 cells in a 96-well plate were infected with these samples. VSVΔG*G was used as a control in most experiments. After 24 h of incubation, each infectious titer was determined as described above.

2.10. Enzymatic and chemical modification of target cells

HepG2 cells in a 96-well plate were washed with PBS and treated with 50 μl of heparitinase (Sigma) for 1 hr, 50 μl of trypsin (Sigma) for 5 min, or 50 μl of α-mannosidase (Sigma) for 1 hr at 37 °C. Subsequently, an equal volume of complete medium was added to stop the enzyme, and then, the cells were washed with PBS and infected with each pseudotype virus sample. HepG2 cells in a 96-well plate were also preincubated in DMEM containing tunicamycin (Sigma) overnight. Then, they were infected with each virus. After 24 h of incubation, the infectious titer was determined.

All the virus titration experiments were done in triplicate. In each figure, the results shown are means, with error bars representing standard deviations (S.D.).

3. Results

3.1. Localization of HCV envelope proteins expressed in 293T cells

We expressed the HCV envelope proteins by transfection with plasmid vectors encoding HCV envelope proteins shown in Table 1. The carboxyl-terminal domains of HCV envelope proteins, E1 and E2, contain ER retention signals [28–30]. To incorporate HCV envelope proteins into VSV particles, it has been reported to be necessary to express these proteins on the cell surface. Thus, to generate HCV pseudotype viruses, chimeric proteins of the ectodomain of HCV E1 or E2, and

Table 1
Detection of HCV envelope proteins by indirect immunofluorescence

Transfected plasmids	Positively stained cells (%)[a]			
	anti-E1		anti-E2	
	(–)[b]	(+)	(–)	(+)
pCXbsr	0	0	0	0
pCXbsr/CE1E2	0	30	0	30
pCXbsr/E1	0	40	0	0
pCXbsr/E2	0	0	0	40
pCXbsr/E1 and pCXbsr/E2	0	40	0	30
pCXbsr/E1, pCXbsr/E2 and pCXbsr/C	0	20	0	30
pCXbsr/E1TM	40	40	0	0
pCXbsr/E2TM	0	0	50	50
pCXbsr/E1TM and pCXbsr/E2TM	30	30	40	40

[a] A mouse monoclonal antibody to E1, E1-384, and a rat monoclonal antibody to E2, Mo-12, were used at a 1/1000 dilution. Percentage of positively stained cells is the mean value from at least three different experiments.

[b] 293T cells were transfected with the indicated plasmid DNA and cultivated for 2 days. The cells were fixed with 4% paraformaldehyde and permeabilized (+), or not (–), with Triton X-100, before immunofluorescence.

the transmembrane domain of VSV G have been used [15–17]. We also made pCXbsr/E1TM and pCXbsr/E2TM encoding the ectodomains of E1 and E2, respectively, joined to the signal sequence, transmembrane and cytoplasmic tail of VSV G protein. In addition, we made plasmid vectors, pCXbsr/CE1E2 coding for the entire HCV structural protein, pCXbsr/C, pCXbsr/E1 and pCXbsr/E2. The structural protein, CE1E2, will be cleaved by cellular signal peptidases [7,8]. Then, we examined the localization of the HCV envelope proteins by indirect immunofluorescence after the fixation of cells with paraformaldehyde (Table 1). Triton X-100-permeabilized cells and non-permeabilized cells were analyzed in parallel. The native forms of the HCV envelope proteins were apparently detected in the transduced cells only after permeabilization. In contrast, the chimeric proteins E1TM and E2TM were observed in both non-permeabilized and permeabilized cells, as reported [16,17].

3.2. Preparation of VSV pseudotypes bearing HCV envelope proteins

3.2.1. Western blotting for HCV envelope proteins

First, to examine whether the native forms of HCV envelope proteins expressed in the cytoplasm in 293T cells could be incorporated into VSV lacking G protein but expressing GFP, VSVΔG* pseudotype virus samples were analyzed by Western blotting (Fig. 2a). E1 was detected as a broad band in a MW range of 30–40 kDa, as previously reported [31,32]. E1 protein in VSVΔG*(HCV) preparation migrated more slowly than E1 protein in VSVΔG*(E1) preparation upon SDS-PAGE. This observation may be explained by different glycosylation of E1 proteins: the glycosylation of E1 has been reported to be enhanced when E1 and E2 are expressed in *cis* [33]. E2 was detected as a discrete band in a MW range of 50–60 kDa, as previously reported [31]. E2 migrated slightly

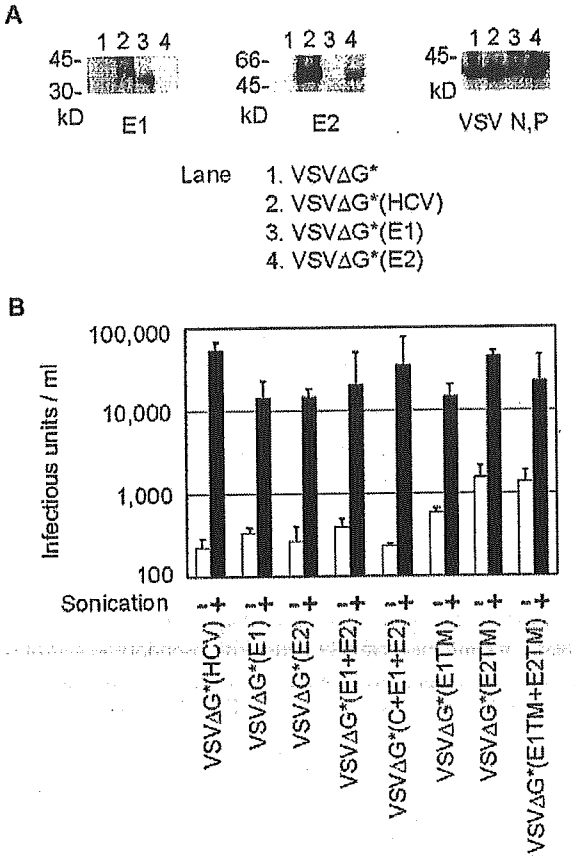

Fig. 2. (a) Western blot analyses of the pseudotype VSVs bearing HCV envelope proteins. Immunoblots of pseudotype virus samples through 20% sucrose cushions are shown. The preparation of each pseudotype sample is described in Table 2. E1 and E2 glycoproteins were detected with E1-384 and Mo-12 monoclonal antibodies against E1 [26] and E2 [27], respectively. VSV proteins were detected by polyclonal goat antibody. The positions of the molecular mass markers (kDa) are shown. (b) Effect of sonication on HCV pseudotype detection. VSV pseudotypes complemented with HCV envelope proteins were prepared after sonication (+, filled column) or without sonication (–, open column). HepG2 cells were infected with the indicated pseudotype viruses, and the IU were determined using the number of GFP-positive cells detected after 24 h of incubation.

faster than E2 reported in other studies [7,16]; this may be due to a variation in glycosylation of E2 among different HCV strains [31,34]. E1 and E2 bands were also detected in VSVΔG*(E1 + E2) or VSVΔG*(C + E1 + E2) samples (data not shown). Bands for the VSV structural proteins N and P with similar intensities were detected in all the four purified pseudotype samples by Western blotting, indicating that similar amounts of VSV were present there. As a control, 293T cells were transfected with E1 and/or E2 vectors but were not infected with VSVΔG*G later. Culture supernatants and cells were harvested, sonicated and subjected to ultracentrifugation, as described above. This sample was also analyzed by Western blotting, and neither E1 nor E2 was detected (data not shown). All these findings suggested the incorporation of the native forms of E1 and/or E2 into VSVΔG* viral particles.

Table 2
Designation of VSV pseudotype samples complemented with HCV glycoproteins

Pseudotype sample[a]	Plasmids
VSVΔG*G	pCAGGS/VSV-G
VSVΔG*(HCV)	pCXbsr/CE1E2
VSVΔG*(E1)	pCXbsr/E1
VSVΔG*(E2)	pCXbsr/E2
VSVΔG*(E1 + E2)	pCXbsr/E1 and pCXbsr/E2
VSVΔG*(C + E1 + E2)	pCXbsr/E1, pCXbsr/E2 and pCXbsr/C
VSVΔG*(E1TM)	pCXbsr/E1TM
VSVΔG*(E2TM)	pCXbsr/E2TM
VSVΔG*(E1TM + E2TM)	pCXbsr/E1TM and pCXbsr/E2TM
VSVΔG*[b]	PCXbsr

[a] VSV pseudotype samples were generated by transfection of cells with the indicated plasmids (total amount of DNA 2 μg per dish) and then by infection of the cells with VSVΔG*G 2 days later. Culture supernatants and the cells were harvested on the following day to prepare pseudotype samples, and stocked at −80 °C after sonication.

[b] VSVΔG* was recovered from cells transfected with pCXbsr plasmid containing no envelope glycoprotein.

3.2.2. *Effect of sonication on pseudotype virus preparation*

Next, we infected HepG2 cells with pseudotype samples that had been prepared with or without sonication. A large number of cells expressed GFP when the cells had been infected with the sonicated sample designated VSVΔG*(HCV), although much fewer cells expressed GFP when infected with the non-sonicated VSVΔG*(HCV) sample (Fig. 2b). The infectivities of other samples, i.e. VSVΔG*(E1), VSVΔG*(E2), VSVΔG*(E1 + E2), VSVΔG*(C + E1 + E2), VSVΔG*(E1TM), VSVΔG*(E2TM) and VSVΔG*(E1TM + E2TM), shown in Table 2, were also examined. The sonication procedure also enhanced their infectivities, as shown in Fig. 2b. In general, the infectivities of the virus samples that could bear the native forms of HCV envelope proteins were enhanced about 100-fold by sonication. With regard to VSVΔG*(E1TM), VSVΔG*(E2TM) and VSVΔG*(E1TM + E2TM), sonication enhanced these pseudotype titers about 10-fold (Fig. 2b).

3.3. *Neutralization of the pseudotype viruses*

To ascertain whether the infectivity of the VSV samples that could contain VSV pseudotypes was specific for the HCV envelope proteins, we examined whether the pseudotype virus activities could be inhibited by treatment with human sera as well as with bovine lactoferrin. While the anti-VSV antibody neutralized VSVΔG*G completely, it did not affect infection with VSVΔG*(HCV) at all (Fig. 3a). Infections of the other HCV pseudotype viruses were not affected by anti-VSV either (data not shown). These results suggested that the HCV envelope proteins conferred envelopes for VSVΔG*. None of the serum samples from 20 chronically HCV-infected Japanese patients, however, exhibited significant neutralization of HCV (E1E2), E1, or E2 pseudotype virus (data not shown). Previously, it was reported that serum samples from a majority of patients with chronic HCV infection failed to show detectable neutralization activity [19].

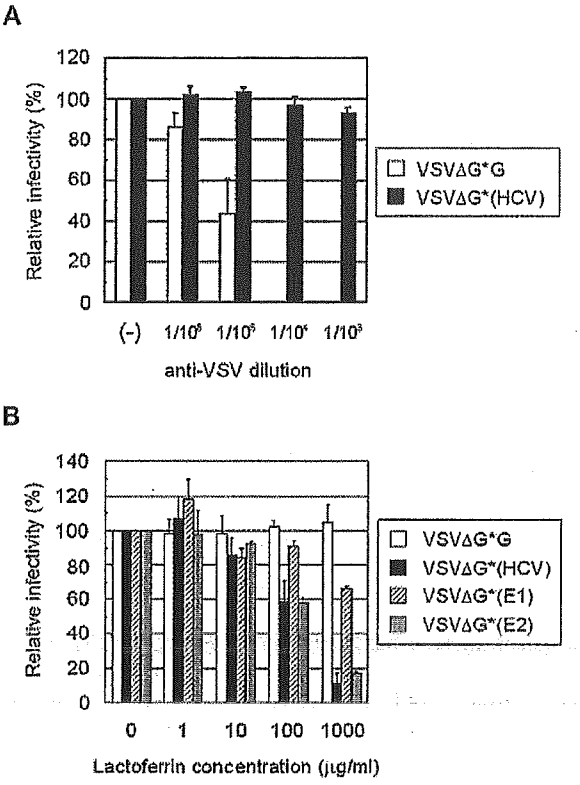

Fig. 3. (a) Neutralization of the pseudotype viruses. Two hundred IU of VSVΔG*(HCV) and VSVΔG*G was preincubated with the indicated dilutions of polyclonal antibody against VSV for 30 min and then inoculated to HepG2 cells. (b) Effect of bovine lactoferrin on the infectivity of pseudotype viruses. Each pseudotype virus (400 IU) was preincubated with various concentrations of bovine lactoferrin for 1 h and then inoculated to HepG2 cells for 1.5 h. Subsequently, the cells were washed with DMEM three times and maintained in culture medium. After 24 h of incubation, relative infectivity (%) was calculated by counting GFP-positive cells. The experiment was done in triplicate, and mean ± S.D. are shown.

3.4. *Effect of bovine lactoferrin on the infectivity of the pseudotype viruses*

We have reported, using PCR, that bovine lactoferrin prevents HCV infection in vitro [20,21]. As HCV-positive human sera were ineffective in inhibiting infection, to support the notion that HCV envelope-specific pseudotypes were formed, we examined whether we could show a specific interaction between lactoferrin and HCV pseudotype samples. Namely, each pseudotype sample was preincubated with various concentrations of lactoferrin, and then HepG2 cells were infected with them. The infectivities of the VSVΔG*(HCV) and VSVΔG*(E2) samples were reduced by preincubation with bovine lactoferrin in a dose-dependent manner, whereas VSVΔG*G was not inhibited (Fig. 3b). VSVΔG*(E1) was only slightly inhibited. This finding is consistent with the report that lactoferrin binds more specifically to E2 than E1 [35].

3.5. Susceptibility of various human cell lines to HCV pseudotypes

Next, we examined the susceptibility of various cell lines to the VSVΔG*(HCV) sample, using VSVΔG*G or VSVΔG* as a control (Table 3). VSVΔG* was prepared without supplying any envelope proteins and showed hardly any infectious titers. Hepatic cell lines, such as HepG2 and Huh7 cells, as well as 293T cells, showed a high susceptibility, and PH5CH8 cells showed a moderate susceptibility to VSVΔG*(HCV). Brain tumor-derived cell lines and primary brain-derived cells were moderately susceptible. Most hematopoietic cell lines were completely resistant to the pseudotype, while MT-2, a human T-cell leukemia virus type I (HTLV-I)-infected T cell line, and HEL, a human erythroleukemia cell line, showed a marginal susceptibility. MT-2 cells as well as HepG2 and PH5CH8 cells that have been reported to be susceptible to HCV infection [36] were susceptible to the VSVΔG*(HCV) sample, suggesting that VSV pseudotypes bearing HCV envelopes were formed.

The susceptibility of various types of cells shown in Table 3 to VSVΔG*(C + E1 + E2) or VSVΔG*(E1TM + E2TM) was also examined comparatively (Table 4). In hepatic cell lines, VSVΔG*(C + E1 + E2) and VSVΔG*(E1TM + E2TM) were nearly as infectious as VSVΔG*(HCV). Onto non-hepatic cells such as 293T, HBMEC or MT-2, VSVΔG*(HCV) plated

Table 3
Infectivity of pseudotype viruses in various human cells

Target	Origin	Pseudotype virus[a]			
		VSVΔG*(HCV)		VSVΔG*G	VSVΔG*
		IU/ml[b]	Ratio[c]	IU/ml	IU/ml
HepG2	Hepatoblastoma	53,000	1	3.4×10^8	280
Huh7	Hepatoma	25,000	0.47	1.2×10^9	1200
PH5CH8	Liver	4700	0.09	2.8×10^9	<10
293T	Embryonal kidney	50,000	0.94	6.8×10^8	300
HUK-1	Kidney	800	0.02	7.2×10^{10}	40
A172	Glioma	19,000	0.36	1.3×10^8	80
NP2	Glioma	15,000	0.28	2.6×10^8	<10
U251	Glioma	2200	0.04	1.1×10^9	<10
U87MG	Glioblastoma	1100	0.02	9.8×10^7	120
HBMEC	Brain microvascular endothelial cell	3600	0.07	3.1×10^8	100
HBP	Brain pericyte	520	0.01	2.8×10^7	60
HOS	Osteosarcoma	1500	0.03	1.0×10^7	20
Molt-4	T-cell acute lymphocytic leukemia	<10		1.2×10^9	<10
TALL-1	T-cell acute lymphocytic leukemia	40		3.2×10^8	<10
C8166	HTLV-1 (+) T cells	<10		8.0×10^8	<10
C91/PL	HTLV-1 (+) T cells	<10		2.0×10^8	100
MT-2	HTLV-1 (+) T cells	260	0.005	8.0×10^8	<10
BALL-1	B-cell acute lymphocytic leukemia	<10		1.7×10^8	<10
Daudi	Burkitt's lymphoma	<10		4.2×10^8	<10
Raji	Burkitt's lymphoma	<10		3.6×10^8	<10
Wil2NS	Plasmacytoma	20		5.2×10^8	<10
HEL	Erythroleukemia	240	0.005	1.4×10^9	<10
K562	Chronic myelogenous leukemia	40		2.8×10^8	20
HL-60	Acute promyelocytic leukemia	<10		4.2×10^7	20
U937	Histiocytic leukemia	<10		6.1×10^8	<10

[a] Pseudotype virus samples described in Table 2 were diluted and inoculated onto the indicated cells.
[b] Infectious units/ml (IU/ml) were determined by counting the number of GFP-expressing cells under a fluorescence microscope after 24 h infection. The experiments were done in triplicate, and means are shown.
[c] The relative ratio of infectious titers compared to HepG2 cells are shown.

Table 4
Infectivity of various HCV pseudotype viruses in human cells

Pseudotype virus[a]	IU/ml	Relative infectivity						
	HepG2	HepG2	Huh7	PH5CH8	293T	A172	NP2	HBMEC	MT-2
VSVΔG*(HCV)	53,000[b]	1[c]	0.47	0.09	0.94	0.36	0.28	0.07	0.005
VSVΔG*(C + E1 + E2)	35,000	1	0.40	0.05	0.45	0.19	0.10	0.01	0.001
VSVΔG*(E1TM + E2TM)	22,000	1	0.50	0.09	0.68	0.30	0.20	0.01	<0.001

The experiments were done in triplicate, and means are shown.
[a] Pseudotype virus samples described in Table 2 were diluted and inoculated onto the indicated cells.
[b] Infectious units/ml (IU/ml) were determined by counting the number of GFP-expressing cells under a fluorescence microscope after 24 h infection.
[c] The relative ratios of infectious titers to HepG2 cells are shown.

much more efficiently than VSVΔG*(C + E1 + E2) and VSVΔG*(E1TM + E2TM): these two latter pseudotypes were prepared with E1 and E2 expressed in *trans*.

3.6. Effect of sulfated polysaccharides on pseudotype virus infection

The infection of several flaviviruses, such as Japanese encephalitis virus and dengue virus serotype 2, has been reported to be inhibited by sulfated polysaccharides, especially heparan sulfate [37,38]. To investigate whether proteoglycans are involved in HCV infection, we examined the plating of VSVΔG*(HCV) and VSVΔG*G on HepG2 cells treated with heparitinase. Fig. 4a shows that heparitinase treatment of the cells reduced the plating of VSVΔG*(HCV). Next, we examined effects of highly sulfated polysaccharides, heparin, dextran sulfate (MW 8000 or 500,000), and unsulfated dextran (MW 7000) on VSVΔG*(HCV) infection (Fig. 4b). Heparin and sulfated dextrans effectively blocked VSVΔG*(HCV) infection, while unsulfated dextran was completely inactive in inhibiting VSVΔG*(HCV) infection. In contrast, the infectivity of VSVΔG*G was hardly affected by sulfated polysaccharides (data not shown).

To examine whether the sulfation level affected VSVΔG*(HCV) infection, sodium chlorate-treated HepG2 cells were infected with VSVΔG*(HCV), because sodium chlorate acts as a sulfate analog and reduces the sulfation level of cellular proteins and glycosaminoglycans (GAGs) [39,40]. Treatment of HepG2 cells with sodium chlorate reduced the VSVΔG*(HCV) titer by about 50% (data not shown). These results suggested that highly sulfated forms of the cell surface GAGs play roles in VSVΔG*(HCV) infection.

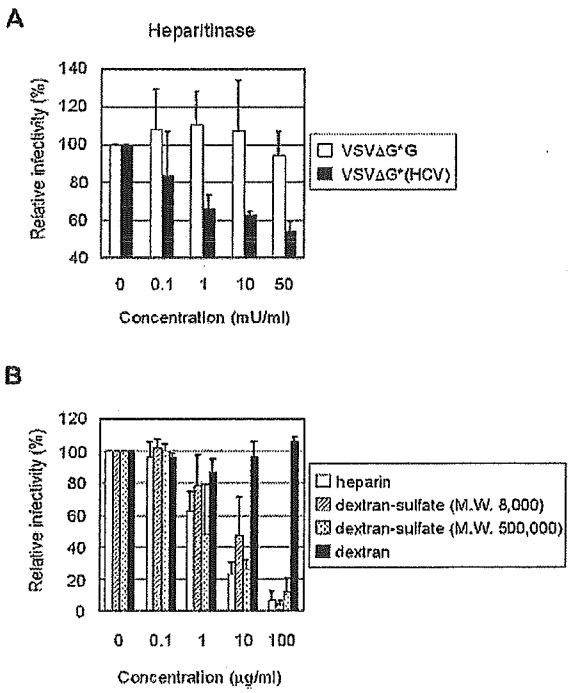

Fig. 4. Effects of sulfated polysaccharides on pseudotype infection. (a) Effect of heparitinase on infectivity of VSVΔG*(HCV). HepG2 cells were treated with various concentrations of heparitinase. The treated cells were infected with 200 IU of VSVΔG*(HCV) or VSVΔG*G. (b) Effect of sulfated polysaccharides on the infectivity of VSVΔG*(HCV). Two hundred IU of VSVΔG*(HCV) was preincubated with heparin, dextran sulfate or dextran at various concentrations for 1 h and then inoculated to HepG2 cells. After 24 h of incubation, the infectivity of the viruses was evaluated. The experiment was done in triplicate, and mean ± S.D. are shown.

3.7. Effects of enzymatic or chemical modification of the target cells on the plating of the HCV pseudotype

To characterize cellular factors necessary for HCV entry, we examined the plating of VSVΔG*(HCV) on HepG2 cells treated with various chemicals. Trypsin treatment of cells markedly reduced the infectivity of VSVΔG*(HCV), while the infectivity of VSVΔG*G was weakly affected (Fig. 5a). Either phospholipase C or sodium periodate marginally reduced the infectivity of VSVΔG*(HCV) (data not shown). Similar results were obtained with 293T cells (data not shown).

Next, the infection of VSVΔG*(HCV) was assessed with inhibitors of protein glycosylation. As shown in Fig. 5b, tunicamycin reduced the plating of VSVΔG*(HCV) by about 90%, whereas castanospermine reduced the infectivity by 20–30%, and neither deoxymannojirimycin nor swainsonine inhibited the plating of VSVΔG*(HCV) (data not shown). α-Mannosidase treatment of cells before infection reduced the infectivity of VSVΔG*(HCV) by about 70% at 500 μg/ml (Fig. 5c). These findings suggested that N-linked glycosylation of a protein(s) on the cell surface might have a role in HCV entry.

4. Discussion

We tried to develop a system to detect the infectivity of recombinant VSV pseudotypes bearing the native forms of HCV envelopes. The co-expression of E1 and E2, or expression of E1 or E2 alone, efficiently complemented the infectivity of VSV lacking the envelope G protein. We used the native forms of the HCV envelope proteins, because we considered that it might be more relevant to examine functions of the HCV envelopes. This system would enable us to study the early stages of HCV infection easily.

There has been no assay system in which infection of HCV has been detected readily and rapidly. For this, VSV pseudotype systems for HCV have been developed by several groups. Because both HCV E1 and E2 have ER retention signals in their C-terminal transmembrane domains, these proteins have been found to be retained in the ER [28–30]. This finding was confirmed by us (Table 1). Therefore, to prepare VSV pseudotypes bearing HCV envelopes, chimeric proteins consisting of carboxy-terminal-truncated HCV envelopes fused to the transmembrane and cytoplasmic tail of VSV G glycoprotein have been used to localize them on the cell surface [15–17]. Baumert et al. [41] reported that HCV-like particle

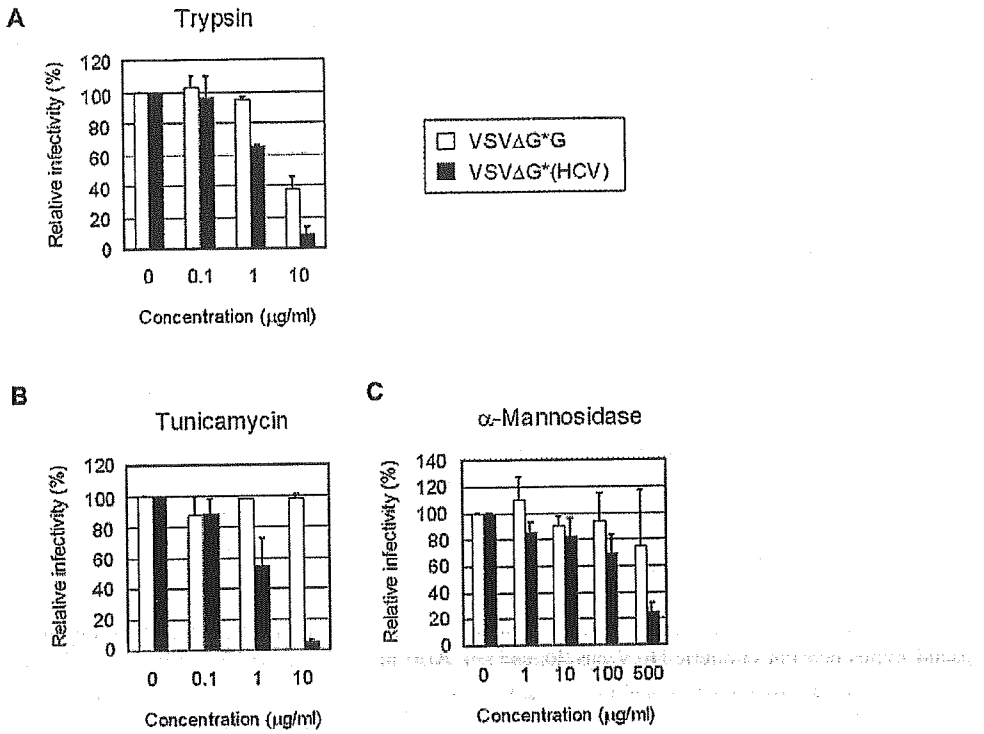

Fig. 5. Infectivity of pseudotype viruses in chemically modified cells. (a) HepG2 cells were preincubated with various concentrations of trypsin for 5 min. Subsequently, an equal volume of complete medium was added to stop the enzyme. Then, the cells were washed and infected with 200 IU of each virus. (b) Effect of glycosylation of cell surface components on the infectivity of VSVΔG*(HCV). HepG2 cells were preincubated with the indicated concentrations of tunicamycin for 24 h. Then, the cells were infected with 200 IU of each virus. (c) Effect of α-mannosidase treatment of cells on the entry of VSVΔG*(HCV). HepG2 cells were preincubated with α-mannosidase at various concentrations for 1 h. Then, the cells were washed and infected with 200 IU of each virus. After 24 h of incubation, the infectivity of the viruses was determined. The experiment was done in triplicate, and mean ± S.D. are shown.

assembly occurs in the cytoplasmic vesicles and that pseudoparticles bearing native HCV envelope proteins will not be released or secreted into culture medium, but accumulate in the ER, like parental HCV virions. There is, however, a possibility that these VSV pseudotype viruses might not exactly reflect the characteristics of the native envelope proteins of viral particles.

HCV virions bearing the native form of HCV envelope proteins should be released from cells in vivo, since plasma samples of HCV-infected humans have frequently shown high infectivity [1,5,42]. It is enigmatic for us how HCV virions have been produced in vivo; nevertheless, both E1 and E2 proteins harbor the ER retention signal. Very recently, Bartosch et al. [43] and Hsu et al. [44] reported the existence of pseudoparticles bearing unmodified HCV envelopes on retroviral core particles. They suggested that a small portion of E1 and E2 would be expressed on the cell surface when these proteins had been expressed abundantly in cells, and thus the retroviral pseudotype bearing E1E2 could be detected. In contrast, we showed that VSV pseudotypes bearing the native form of HCV envelope proteins with highly infectious titers, as compared with previous reports, could be produced by the cells expressing the HCV envelope proteins in the cytoplasm (Table 1 and Fig. 2).

Unlike previous studies [15–17], we thus successfully detected the infectious activities considered to be due to the formation of VSV pseudotype viruses when VSV was complemented with the native forms of HCV envelope proteins. Although only a small amount of pseudotype virus was initially detected in the culture medium, when the harvested pseudotype samples were sonicated for a short time, their titers were enhanced about 100-fold (Fig. 2b). In our assay system, the carryover of VSVΔG*G into HCV pseudotype samples would be minimized by treatment with polyclonal antibody to VSV. Probably due to the efficient decrease in the carryover and the release of pseudotype virions associated with the cell membrane by sonication, we could detect HCV pseudotypes with the native forms of envelopes.

We have reported that bovine and human lactoferrins prevent HCV infection in PH5CH8 human liver cells and MT-2 cells [20,21], and HCV E1 and E2 bind to lactoferrin [35]. We have also reported that the lactoferrin-binding activity of E2 contributes to inhibition of HCV infection [45]. In the present study, pretreatment of VSV pseudotypes with bovine lactoferrin reduced the infectivity of VSVΔG*(HCV) and VSVΔG*(E2) in a dose-dependent manner, whereas pretreatment with transferrin did not (data not shown). In contrast, lactoferrins partially inhibited the infectivity of VSVΔG*(E1) (Fig. 3b). Our results suggested that the interaction between lactoferrin and E2 plays a central role in the inhibition of HCV infection. Taken together, our findings

showed that properties of HCV pseudotypes are consistent with those of HCV virions determined by PCR.

Previously, several groups have demonstrated that not only human hepatic cell lines but also human T cell lines, Molt-4Ma, HPB-Ma, MT-2, and a human B cell line, Daudi, are susceptible to HCV infection [46–49]. In the present study, almost no hematopoietic cell lines were susceptible to any HCV pseudotypes. Only MT-2 and HEL cells showed a marginal susceptibility to the HCV pseudotypes. It is probable that the characteristics of the cell lines might change after long-term cell culture in different laboratories. Interestingly, our results demonstrated that several cell lines derived from the human brain were apparently susceptible to HCV pseudotypes. Encephalomyelitis or encephalitis associated with HCV and cerebral involvement of HCV infection have been reported [50–52]; HCV RNA has been detected in the post-mortem brain and brainstem [53].

Weak immunity against HCV infection has been reported [54]. Recently, it has been documented that serum samples from a majority of patients with chronic HCV infection failed to show a detectable neutralization activity against VSV pseudotypes bearing chimeric HCV envelopes [19]. Also in our study, no significant neutralization of any HCV pseudotypes was observed with serum samples from 20 patients with chronic HCV infection. It should be determined whether neutralizing antibody against E1 or E2 alone can neutralize the VSVΔG*(HCV) pseudotype. If E1 and E2 can function independently and the neutralization of both E1 and E2 is necessary for marked inhibition of HCV infectivity, the development of an effective vaccine or an HCV entry-inhibiting agent will be quite difficult. For detection of neutralizing antibody, it may be necessary to examine patients at the different stages of HCV infection, e.g. acute stage of hepatitis.

Table 4 shows that the three different types of HCV pseudotypes prepared with two HCV envelopes showed only a small difference in infectivity in eight types of cells. As for the difference in infectivity between VSVΔG*(HCV) prepared with structural proteins in *cis* and VSVΔG*(C + E1 + E2) prepared with structural proteins in *trans*, it might be explained by the difference in E1–E2 interaction between them. There are reports that both E1 and E2 are necessary for the efficient formation of VSV or retroviral pseudotypes [17,43,44], while VSV pseudotypes complemented with either E1 or E2 alone have been developed [16]. Our findings also suggest that either E1 or E2 alone is enough to make HCV virions (Fig. 2). Recent study indicates that the presence of the complete HCV core sequence is crucial for the expression and/or post-translational processing of the complex-type glycosylated form of E2 [34], and the glycosylation of E1 is enhanced by coexpression of E2 in *cis* [33]. Our results indicate that the core protein might be required for maximal infectivity of pseudotypes (Fig. 2b). Further studies are needed to clarify the role of each envelope protein in the infection by HCV.

Many viruses including herpes viruses, human immunodeficiency virus, Sindbis virus, and in particular, flaviviruses such as dengue virus serotype 2 and Japanese encephalitis virus utilize proteoglycans, especially heparan sulfate, to mediate attachment to and infection of target cells [37,38,55–57]. Recently, Germi et al. [58] reported that cellular heparin-like GAGs might bind to HCV. Our results suggested that highly sulfated forms of GAGs play a role in the early stage of HCV infection (Fig. 4).

Assays of virus infectivity using chemically modified cells suggest that certain cell surface glycoproteins with N-linked oligosaccharides play an important role in VSVΔG*(HCV) infection (Fig. 5b). In addition, pre-treatment of cells with α-mannosidase suppressed the infectivity of VSVΔG*(HCV) by about 70% (Fig. 5c). Further studies on the surface sugar chain structures of cells will be needed to analyze their roles in the entry of HCV.

In conclusion, our system of producing VSV pseudotypes complemented with the native forms of HCV envelopes will be a useful tool with which to analyze the mechanism for HCV virion formation and the function of HCV envelope proteins. This system may also be an efficient tool for research on HCV entry and its inhibitors.

Acknowledgments

We thank Dr. M.A. Whitt for kindly supplying a VSV G-expressing pCAGGS/VSV-G plasmid and the VSVΔG*G pseudotype. We also thank Dr. M. Kohara for kindly providing us with anti-E1 monoclonal antibody. This work was supported in part by a grant-in-aid from the Japanese Society for the Promotion of Science, grants from the Japan Health Sciences Foundation and CREST, and the 21st century COE program.

References

[1] H.J. Alter, R.H. Purcell, J.W. Shih, J.C. Melpolder, M. Houghton, Q.L. Choo, et al., Detection of antibody to hepatitis C virus in prospectively followed transfusion recipients with acute and chronic non-A, non-B hepatitis, N. Engl. J. Med. 321 (1989) 1494–1500.

[2] M.E. Major, B. Rehermann, S.M. Feinstone, in: D.M. Knipe, P.M. Howley (Eds.), Fields Virology, fourth ed, Lippincott, Philadelphia, PA, 2001, pp. 1127–1161.

[3] M.J. Alter, H.S. Margolis, K. Krawczynski, F.N. Judson, A. Mares, W.J. Alexander, et al., The natural history of community-acquired hepatitis C in the United States, N. Engl. J. Med. 327 (1992) 1899–1905.

[4] I. Saito, T. Miyamura, A. Ohbayashi, H. Harada, T. Katayama, S. Kikuchi, et al., Hepatitis C virus infection is associated with the development of hepatocellular carcinoma, Proc. Natl. Acad. Sci. USA 87 (1990) 6547–6549.

[5] Q.L. Choo, G. Kuo, A.J. Weiner, L.R. Overby, D.W. Bradley, M. Houghton, Isolation of a cDNA clone derived from a blood-borne non-A, non-B viral hepatitis genome, Science 244 (1989) 359–362.

[6] N. Kato, M. Hijikata, Y. Ootsuyama, M. Nakagawa, S. Ohkoshi, T. Sugimura, et al., Molecular cloning of the human hepatitis C virus genome from Japanese patients with non-A, non-B hepatitis, Proc. Natl. Acad. Sci. USA 87 (1990) 9524–9528.

[7] A. Grakoui, C. Wychowski, C. Lin, S.M. Feinstone, C.M. Rice, Expression and identification of hepatitis C virus polyprotein cleavage products, J. Virol. 67 (1993) 1385–1395.

[8] M.J. Selby, Q.L. Choo, K. Berger, G. Kuo, E. Glazer, M. Eckart, et al., Expression, identification and subcellular localization of the proteins encoded by the hepatitis C viral genome, J. Gen. Virol. 74 (1993) 1103–1113.

[9] V. Deleersnyder, A. Pillez, C. Wychowski, K. Blight, J. Xu, Y.S. Hahn, et al., Formation of native hepatitis C virus glycoprotein complexes, J. Virol. 71 (1997) 697–704.

[10] P. Pileri, Y. Uematsu, S. Campagnoli, G. Galli, F. Falugi, R. Petracca, et al., Binding of hepatitis C virus to CD81, Science 282 (1998) 938–941.

[11] E. Scarselli, H. Ansuini, R. Cerino, R.M. Roccasecca, S. Acali, G. Filocamo, C. Traboni, A. Nicosia, R. Cortese, A. Vitelli, The human scavenger receptor class B type I is a novel candidate receptor for the hepatitis C virus, EMBO J. 21 (2002) 5017–5025.

[12] V. Agnello, G. Abel, M. Elfahal, G.B. Knight, Q.X. Zhang, Hepatitis C virus and other flaviviridae viruses enter cells via low density lipoprotein receptor, Proc. Natl. Acad. Sci. USA 96 (1999) 12766–12771.

[13] S. Wunschmann, J.D. Medh, D. Klinzmann, W.N. Schmidt, J.T. Stapleton, Characterization of hepatitis C virus (HCV) and HCV E2 interactions with CD81 and the low-density lipoprotein receptor, J. Virol. 74 (2000) 10055–10062.

[14] F. Masciopinto, G. Freer, V.L. Burgio, S. Levy, L. Galli-Stampino, M. Bendinelli, M. Houghton, S. Abrignani, Y. Uematsu, Expression of human CD81 in transgenic mice does not confer susceptibility to hepatitis C virus infection, Virology 304 (2002) 187–196.

[15] L. Buonocore, K.J. Blight, C.M. Rice, J.K. Rose, Characterization of vesicular stomatitis virus recombinants that express and incorporate high levels of hepatitis C virus glycoproteins, J. Virol. 76 (2002) 6865–6872.

[16] L.M. Lagging, K. Meyer, R.J. Owens, R. Ray, Functional role of hepatitis C virus chimeric glycoproteins in the infectivity of pseudotyped virus, J. Virol. 72 (1998) 3539–3546.

[17] Y. Matsuura, H. Tani, K. Suzuki, T.S. Kimura, R. Suzuki, H. Aizaki, K. Ishii, K. Moriishi, C.S. Robison, M.A. Whitt, T. Miyamura, Characterization of pseudotype VSV possessing HCV envelope proteins, Virology 286 (2001) 263–275.

[18] A. Takada, C. Robison, H. Goto, A. Sanchez, K.G. Murti, M.A. Whitt, et al., A system for functional analysis of Ebola virus glycoprotein, Proc. Natl. Acad. Sci. USA 94 (1997) 14764–14769.

[19] L.M. Lagging, K. Meyer, J. Westin, R. Wejstal, G. Norkrans, M. Lindh, R. Ray, Neutralization of pseudotyped vesicular stomatitis virus expressing hepatitis C virus envelope glycoprotein 1 or 2 by serum from patients, J. Infect. Dis. 185 (2002) 1165–1169.

[20] M. Ikeda, K. Sugiyama, T. Tanaka, K. Tanaka, H. Sekihara, K. Shimotohno, et al., Lactoferrin markedly inhibits hepatitis C virus infection in cultured human hepatocytes, Biochem. Biophys. Res. Commun. 245 (1998) 549–553.

[21] M. Ikeda, A. Nozaki, K. Sugiyama, T. Tanaka, A. Naganuma, K. Tanaka, et al., Characterization of antiviral activity of lactoferrin against hepatitis C virus infection in human cultured cells, Virus Res. 66 (2000) 51–63.

[22] R.B. DuBridge, P. Tang, H.C. Hsia, P.M. Leong, J.H. Miller, M.P. Calos, Analysis of mutation in human cells by using an Epstein–Barr virus shuttle system, Mol. Cell. Biol. 7 (1987) 379–387.

[23] M. Ikeda, K. Sugiyama, T. Mizutani, T. Tanaka, K. Tanaka, H. Sekihara, et al., Human hepatocyte clonal cell lines that support persistent replication of hepatitis C virus, Virus Res. 56 (1998) 157–167.

[24] T. Akagi, T. Shishido, K. Murata, H. Hanafusa, v-Crk activates the phosphoinositide 3-kinase/AKT pathway in transformation, Proc. Natl. Acad. Sci. USA 97 (2000) 7290–7295.

[25] H. Niwa, K. Yamamura, J. Miyazaki, Efficient selection for high-expression transfectants with a novel eukaryotic vector, Gene 108 (1991) 193–199.

[26] T. Wakita, C. Taya, A. Katsume, J. Kato, H. Yonekawa, Y. Kanegae, et al., Efficient conditional transgene expression in hepatitis C virus cDNA transgenic mice mediated by the cre/loxP system, J. Biol. Chem. 273 (1998) 9001–9006.

[27] M. Inudoh, N. Kato, Y. Tanaka, New monoclonal antibodies against a recombinant second envelope protein of hepatitis C virus, Microbiol. Immunol. 42 (1998) 875–877.

[28] L. Cocquerel, J.C. Meunier, A. Pillez, C. Wychowski, J. Dubuisson, A retention signal necessary and sufficient for endoplasmic reticulum localization maps to the transmembrane domain of hepatitis C virus glycoprotein E2, J. Virol. 72 (1998) 2183–2191.

[29] L. Cocquerel, S. Duvet, J.C. Meunier, A. Pillez, R. Cacan, C. Wychowski, et al., The transmembrane domain of hepatitis C virus glycoprotein E1 is a signal for static retention in the endoplasmic reticulum, J. Virol. 73 (1999) 2641–2649.

[30] L. Cocquerel, C. Wychowski, F. Minner, F. Penin, J. Dubuisson, Charged residues in the transmembrane domains of hepatitis C virus glycoproteins play a major role in the processing, subcellular localization, and assembly of these envelope proteins, J. Virol. 74 (2000) 3623–3633.

[31] H.J. Ezelle, D. Markovic, G.N. Barber, Generation of hepatitis C virus-like particles by use of a recombinant vesicular stomatitis virus vector, J. Virol. 76 (2002) 12325–12334.

[32] B. Bartosch, A. Vitelli, C. Granier, C. Goujon, J. Dubuisson, S. Pascale, E. Scarselli, R. Cortese, A. Nicosia, F.L. Cosset, Cell entry of hepatitis C virus requires a set of co-receptors that include the CD81 tetraspanin and the SR-IB scavenger receptor, J. Biol. Chem. 278 (2003) 41624–41630.

[33] A. Goffard, J. Dubuisson, Glycosylation of hepatitis C virus envelope proteins, Biochimie 85 (2003) 295–301.

[34] L.X. Zhu, L. Liu, Y.C. Li, Y.Y. Kong, C. Staib, G. Sutter, Y. Wang, G.D. Li, Full-length core sequence dependent complex-type glycosylation of hepatitis C virus E2 glycoprotein, World J. Gastroenterol. 8 (2002) 499–504.

[35] M. Yi, S. Kaneko, D.Y. Yu, S. Murakami, Hepatitis C virus envelope proteins bind lactoferrin, J. Virol. 71 (1997) 5997–6002.

[36] N. Kato, M. Ikeda, K. Sugiyama, T. Mizutani, T. Tanaka, K. Shimotohno, Hepatitis C virus population dynamics in human lymphocytes and hepatocytes infected in vitro, J. Gen. Virol. 79 (1998) 1859–1869.

[37] Y. Chen, T. Maguire, R.E. Hileman, J.R. Fromm, J.D. Esko, R.J. Linhardt, et al., Dengue virus infectivity depends on envelope protein binding to target cell heparan sulfate, Nat. Med. 3 (1997) 866–871.

[38] C.M. Su, C.L. Liao, Y.L. Lee, Y.L. Lin, Highly sulfated forms of heparin sulfate are involved in Japanese encephalitis virus infection, Virology 286 (2001) 206–215.

[39] P.A. Baeuerle, W.B. Huttner, Chlorate—a potent inhibitor of protein sulfation in intact cells, Biochem. Biophys. Res. Commun. 141 (1986) 870–877.

[40] F. Safaiyan, S.O. Kolset, K. Prydz, E. Gottfridsson, U. Lindahl, M. Salmivirta, Selective effects of sodium chlorate treatment on the sulfation of heparan sulfate, J. Biol. Chem. 274 (1999) 36267–36273.

[41] T.F. Baumert, S. Ito, D.T. Wong, T.J. Liang, Hepatitis C virus structural proteins assemble viruslike particles in insect cells, J. Virol. 72 (1998) 3827–3836.

[42] G. Kuo, Q.L. Choo, H.J. Alter, G.L. Gitnick, A.G. Redeker, R.H. Purcell, et al., An assay for circulating antibodies to a major etiologic virus of human non-A, non-B hepatitis, Science 244 (1989) 362–364.

[43] B. Bartosch, J. Dubuisson, F.L. Cosset, Infectious hepatitis C virus pseudo-particles containing functional E1–E2 envelope protein complexes, J. Exp. Med. 197 (2003) 633–642.

[44] M. Hsu, J. Zhang, M. Flint, C. Logvinoff, C.C. Mayer, C.M. Rice, J.A. McKeating, Hepatitis C virus glycoproteins mediate pH-dependent cell entry of pseudotyped retroviral particles, Proc. Natl. Acad. Sci. USA 100 (2003) 7271–7276.

[45] A. Nozaki, M. Ikeda, A. Naganuma, T. Nakamura, M. Inudoh, K. Tanaka, N. Kato, Identification of a lactoferrin-derived peptide possessing binding activity to hepatitis C virus E2 envelope protein, J. Biol. Chem. 278 (2003) 10162–10173.